Chapter 1

SCIENTIFIC HIGHLIGHTS

OUTFLOWS FROM AGNS ORIGINATE AS DISK WINDS ORBITING A SUPER-MASSIVE BLACK HOLE

Most galaxies undergo an active phase, during which a central super-massive black hole generates vast radiant luminosities through the gravitational accretion of gas. Winds launched from a rotating accretion disk surrounding the black hole are thought to play a critical role, allowing the disk to shed angular momentum that would otherwise inhibit accretion. Such winds are capable of depositing large amounts of mechanical energy in the host galaxy and its environs, profoundly affecting its formation and evolution, and perhaps regulating the formation of large-scale cosmological structures in the early Universe. However, observational verification that AGN outflows originate as disk winds has proven elusive.

Using the ISIS spectrograph in its spectropolarimetric mode on the WHT, a team of astronomers was able to obtain the first observational evidence that indeed outflows from active galactic nuclei originate as winds from rotating accretion disks surrounding a super-massive black hole. The evidence came from observations of the quasar PG 1700+518 and some of the results can be seen in Figure 1.

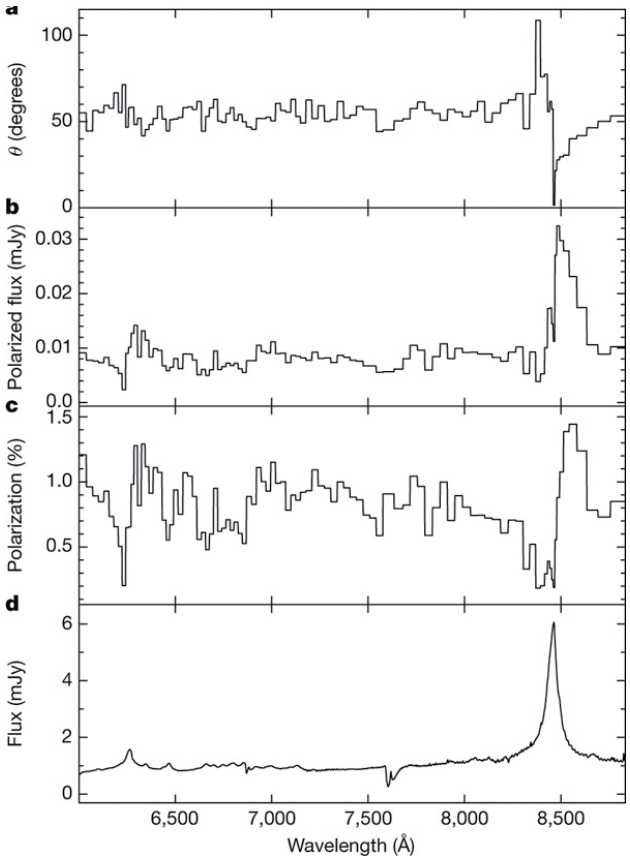

Figure 1. The polarisation data for the BAL quasar PG1700+518. The data were obtained using ISIS spectrograph on the WHT, at a spectral resolution of 3.4 Å. The polarisation data have been re-sampled into bins with an error of 0.1% in degree of polarisation. a) The position angle of polarisation, θ; b) the polarised flux spectrum in mJy; c) the degree of polarisation as a percentage; and d) the total flux spectrum in mJy. Note the large change in polarisation position angle across the broad Hα emission line, which reverses direction at the line peak. In polarised flux, the broad emission line is redshifted with respect to the wavelength of the peak in total flux. Adapted with permission from Macmillan Publishers Ltd: Nature (S. Young et al., 450, 74), copyright 2007.

A GIANT OUTBURST TWO YEARS BEFORE THE CORE-COLLAPSE OF A MASSIVE STAR

For the first time, astronomers witnessed a double stellar explosion at exactly the same position on the sky, suggesting the death of a massive star.

SN 2006jc was discovered in UGC 4904 on 2006 October 9. The early spectrum was that of a hydrogen-poor event with strong, narrow He I emission lines superimposed on a broad-line spectrum of a type Ic supernova. In 2004, an optical transient was reported which, when retrospectively compared with the SN 2006jc discovery images, appeared to be spatially coincident with the supernova. The 2004 transient was much fainter than SN 2006jc and it remained visible for only a few days after discovery. Given the new bright supernova discovery, the nature of this transient, named UGC 4904-V1, became intriguing.

A global collaboration of astronomers analysed the images containing the two transients using differential astrometry of 21 nearby stars, and found that UGC 4904-V1 and SN 2006jc were indeed coincident to within the uncertainties. So they decided to follow-up and study SN2006jc with a

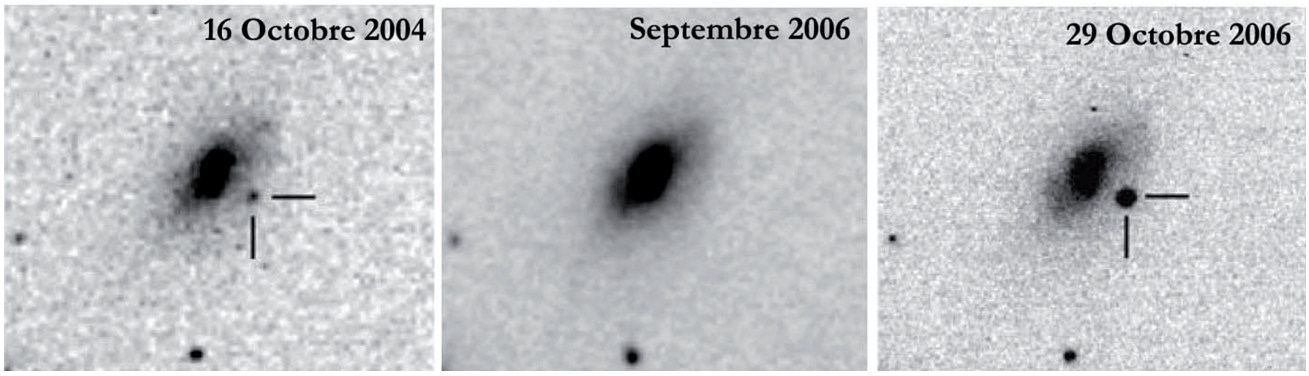

Figure 2. Sequence of images of UGC 4904 rebinned to a pixel scale of 0.53 arcsec. Left: detection of UGC 4904-V1 on 2004 October 16. Middle: another image obtained on 2006 September 21 showing no transient detection. Right: R-band frame taken on 2006 October 29. The two transients are coincident to within 0.1 arcsec, and the total error budget is 0.3 arcsec. Adapted with permission from Macmillan Publishers Ltd: Nature (Pastorello, A. et al., 447, 829), copyright 2007.

wide range of large telescopes, among them the WHT and its ISIS spectrograph.

The most likely explanation for the 2004 explosion is a giant outburst of a very massive star like Eta-Carinae, and only the most massive stars can produce this type of outburst. So the 2006 supernova must have been the death of the same star, possibly one that was 50 to 100 times more massive than the Sun. It turns out that SN2006jc is a very weird supernova – unusually rich in the chemical element helium, which supports the idea of a massive star outburst, followed by death.

THE MOST DETAILED IMAGE EVER PRODUCED OF THE ROSETTE NEBULA

Compiled from data taken from IPHAS, the Isaac Newton Telescope Photometric Hα Survey of the Northern Galactic Plane, astronomers produced a new image of the Rosette Nebula (NGC 2237) which is thought to be the most-detailed ever produced. The image spans four square degrees, about twenty times the size of the full moon.

The Rosette Nebula is a vast cloud of dust and gas spanning 100 light years and lying about 4500 light-years away. Inside the nebula lies a cluster of bright massive stars (NGC 2244), whose strong stellar winds and radiation have cleared a hole in the nebula's centre. Ultraviolet light from these hot stars excites the surrounding nebula, causing it to glow.

Star formation is still active around the nebula, as proven by the presence of a very young infrared star (AFGL 961) still in its final stages of formation. It is thought that the young massive stars in the nebula will one day blow all the gas and dust away. The centre of the Rosette Nebula is about 1.8 degrees below the Galactic Plane, the glow from which can be seen at the top left (north eastern) corner of Figure 3.

Due to its large angular size, most large telescopes are unable to capture the entire nebula in one exposure and therefore the highest resolution images have been limited to small areas. IPHAS is in the process of imaging the entire Galactic Plane and members of the survey team were able to combine almost 200 individual CCD images to make this large and detailed Hα image.

Even more detailed images of the central parts of the Rosette Nebula have also been prepared by the IPHAS team, including an image of dense dust lanes where star formation may still be ongoing.

IPHAS is a photometric imaging survey of the entire Northern Galactic Plane at three different wavelengths, using the Wide Field Camera on the INT to cover an area of 1800 square degrees. The survey will soon be followed by VPHAS+, a complementary Southern Galactic Plane survey using telescopes in the southern hemisphere.

THE TRANS-NEPTUNIAN OBJECTS 2005 FY_9 AND 2003 UB_{313} ARE SIMILAR TO PLUTO

The discovery of two large trans-Neptunian objects (TNOs) 2003 UB_{313} and 2005 FY_9, with surface properties similar to those of Pluto, provided an exciting new laboratory for the study of processes found in Pluto and Triton: volatile mixing and transport; atmospheric freeze-out and escape, ice chemistry, and nitrogen phase transitions.

Figure 3. Next two pages: The Rosette Nebula as seen in H-alpha light. Image size is 126×115 arcminutes, 1 arcsecond per pixel. North is up, east is to the left. Image credit: Nick Wright (University College London) and the IPHAS collaboration.

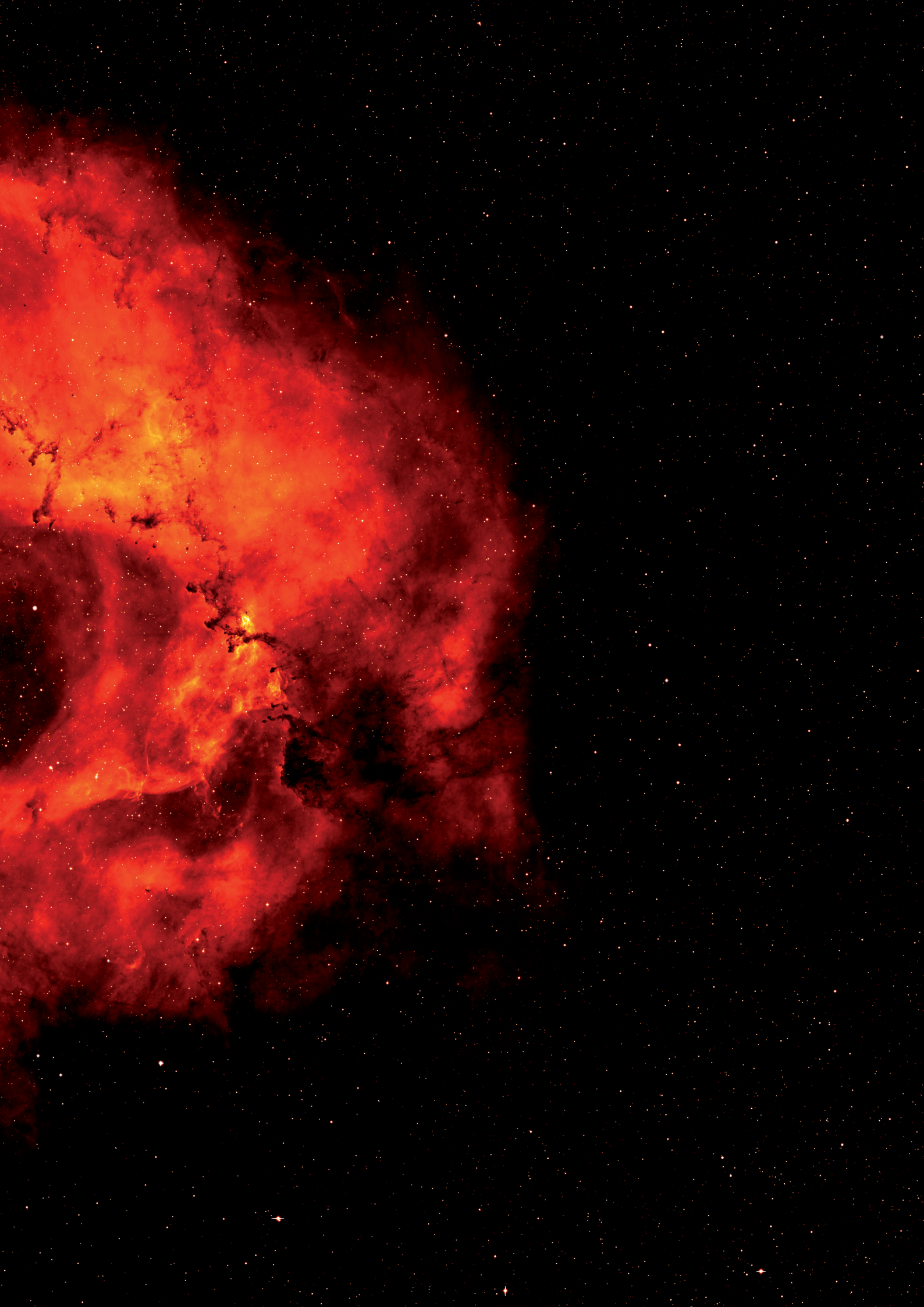

2005 FY_9 is the third brightest known TNO, after 2003 UB_{313} and Pluto. The size of 2005 FY_9 is approximately 0.7 times that of Pluto. The semi-major axis of its orbit is 46 AU, the perihelion distance is 39 AU and the inclination of the orbit is 29°. These values are typical of the classical TNO family.

Visible spectroscopy of 2005FY_9 was obtained using the ISIS spectrograph on the WHT, and near-infrared spectroscopy was obtained using the NICS spectrograph on the TNG. The complete visible and near-infrared spectra were compared with the spectrum of Pluto and that of pure methane ice and it was found that the spectra of both TNOs are very similar. They are dominated by strong absorption bands produced by methane ice. In fact, the absorption bands in the spectrum of 2005 FY_9 are deeper than in the spectrum of Pluto, as a result of the larger abundance of methane ice in 2005 FY_9. Also the colour of the surface of the TNO (indicated by the slope of the spectrum) is red, similar to that of Pluto. This shows the presence of complex organic compounds in the surface.

Until now only one known TNO, Pluto, showed the presence of strong methane ice absorption bands in its spectrum. However, apart from 2005 FY_9, these bands were also recently observed in the spectrum of the largest yet known TNO, 2003 UB_{313}, as shown in the Figure 5. The near infrared spectrum of 2003 UB_{313} is very similar to that of 2005 FY_9.

The visible spectrum of 2003 UB_{313} shows very prominent absorption bands from solid CH_4. The icy-CH_4 bands are significantly stronger than those of Pluto and slightly weaker than those observed in the spectrum of 2005 FY_9. A shift relative to the position of the bands in the spectrum of laboratory CH_4 ice is observed in the bands at larger wavelengths, but not at shorter wavelengths, which can be explained by a vertical compositional gradient. Purer methane could have condensed first, while 2003 UB_{313} moved towards aphelion during the last 200 years: as the atmosphere gradually collapsed, the composition became more nitrogen-rich due to the fact that most volatile components condensed and CH_4 diluted in N_2, present in the outer surface layers.

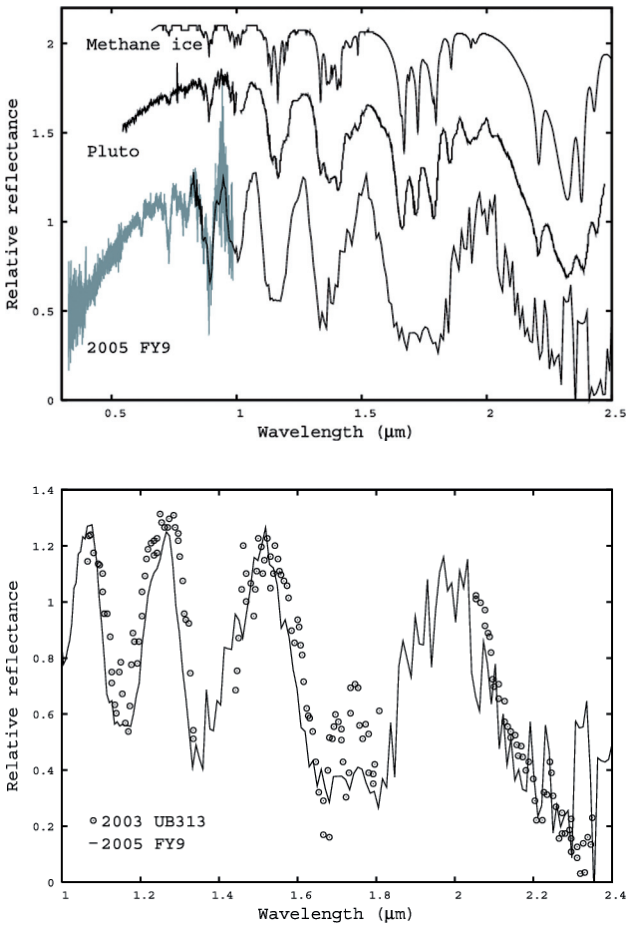

Figure 4. Top: The spectrum of 2005 FY_9 compared with the spectrum of Pluto and that of pure methane ice. Notice the strong methane ice absorption bands present in the spectrum of both TNOs. Bottom: Near infrared spectrum of 2005 FY_9 compared with that of TNO 2003 UB313. The similarity of both spectra shows that the surface composition of the two objects must be similar (figure from Licandro et al., 2006, A&A, 445, L35).

THE YORP EFFECT DETECTED ON NEAR-EARTH ASTEROID 2000 PH5

The Yarkovsky-O'Keefe-Radzievskii-Paddack (YORP) effect is believed to alter the way small bodies in the solar system rotate. YORP is a torque due to sunlight hitting the surfaces of asteroids and meteoroids and warming their surfaces, leading to a gentle recoil effect as the heat is emitted. By analogy, if one were to shine light on a propeller over a long enough period, it would start spinning.

Although this is an almost immeasurably weak force, astronomers believe it may be responsible for spinning some asteroids up so fast that they break apart, perhaps leading to the formation of binary asteroids. Others may be slowed down so that they take many days to rotate once. The YORP effect also plays an important role in changing the orbits of asteroids between Mars and Jupiter, including their delivery to planet-crossing orbits. Despite its importance, the effect has never been seen acting on a solar system body, until now.

Using extensive optical and radar imaging from powerful Earth-based observatories, astronomers have directly

observed the YORP effect in action on a small near-Earth asteroid, known as (54509) 2000 PH5.

Shortly after its discovery in 2000, it was realised that this asteroid would be the ideal candidate for such a YORP detection. At just 114m in diameter, it is relatively small and so more susceptible to the effect. Also, it rotates very quickly, with one day on the asteroid lasting just over 12 Earth minutes, implying that the YORP effect may have been acting on it for some time. With this in mind, the team of radar and optical astronomers undertook a long term monitoring campaign of the asteroid, with the aim of detecting any tiny changes in the spin-rate.

Over a 4 year time span, astronomers took images of the asteroid at a range of telescope sites including the INT. With these facilities the astronomers measured the slight brightness variations as the asteroid rotated.

They found that the asteroid is rotating faster by 1 millisecond every year, which is caused by the heating of the asteroid's surface by the Sun. Eventually it may spin faster than any known asteroid in the solar system. Figure 5 shows the change of the rotational period over the years.

COMET 17P/HOLMES OBSERVED WITH THE EYES OF THE INT

On the night of the 23rd of October 2006, Comet 17P/Holmes underwent an outburst that increased its brightness by a factor of a million during the following days.

The INT pointed to the comet just after sunset on the night following the outburst, and it detected a highly centralised condensed coma with no signs of a tail. The coma had

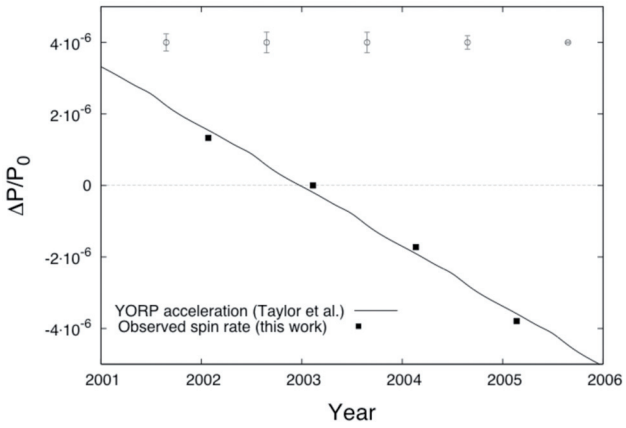

Figure 5. The observed spin-rate was seen to change from year to year (black dots). The solid curve is the expected theoretical YORP strength derived from the 3-D shape model (figure from Lowry et al., 2007, Science, 316, 272).

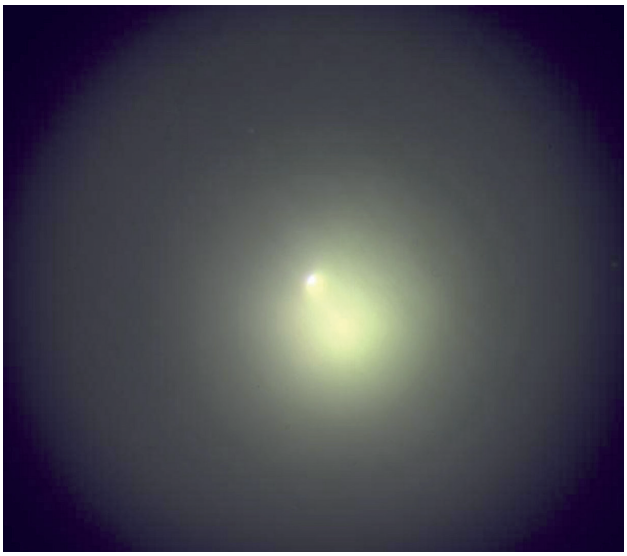

Figure 6. INT image of comet 17P/Holmes processed to show the inner coma structure. Credit: T Naylor / A Fitzsimmons / C Brunt / ING.

extended out to 37,000 km from the nucleus, and the outer edge was almost perfectly circular. This distance implied that the dust was moving at least 0.2 km per second (800 km per hour) from the central nucleus. Image processing showed that the material was currently leaving the comet towards the South East.

Figure 6 shows an expanding circular cloud of gas and dust emanating from the nucleus, together with a brighter cloud of material.

FIRST OBSERVATIONAL EVIDENCE OF A DEAD CATACLYSMIC VARIABLE

A long-standing and unverified prediction of binary star evolution theory is the existence of a population of white dwarfs accreting from substellar donor stars. Such systems ought to be common, but the difficulty of finding them, combined with the challenge of detecting the donor against the light from accretion, means that no donor star to date has a measured mass below the hydrogen burning limit.

A binary star system in which a white dwarf accretes material from a companion is called a cataclysmic variable (CV). Every kilogram of material that falls onto the white dwarf gains the energy equivalent of a few kilotons of TNT. Much of this energy is released as ultraviolet or X-ray radiation. Many CVs have been identified from this highly variable, short-wavelength light produced by rapid mass transfer onto the white dwarf. However, most CVs should have evolved through this violent phase to become a "dead CV" with a low-mass companion that can support

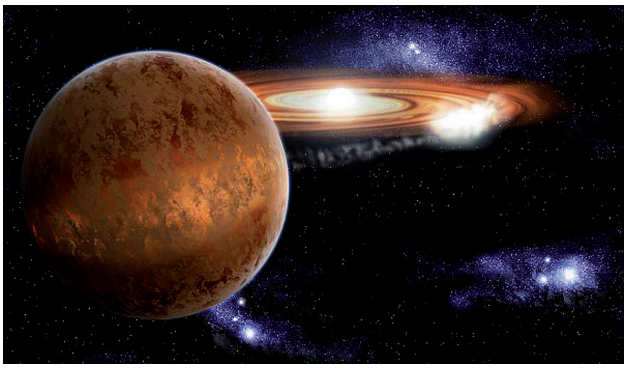

Figure 6. Artist's impression of SDSS 1035+0551. The hot white dwarf is the same size as the Earth, yet its mass is the same as our Sun. The brown dwarf is about the same size as Jupiter, but much more massive. The gravity of the white dwarf pulls gas from the brown dwarf; this gas spirals down onto the surface of the white dwarf, like water down a plughole, forming an accretion disc of hot gas around the white dwarf. Where the falling gas from the brown dwarf hits the accretion disc, it creates a hot spot. The position of this hot spot depends on the masses of the two stars. The authors precisely timed when the white dwarf and hot spot were eclipsed by the brown dwarf. This allowed them to measure the location of the hot spot, and infer the masses of the two stars. Credit: Stuart Littlefair/Science.

only weak mass transfer. Extensive efforts to confirm this long-standing prediction have failed to identify any CVs that have clearly survived the rapid mass transfer phase of their evolution.

A team of astronomers using ULTRACAM on the WHT reported for the first time the unambiguous detection of a dead CV from a direct mass measurement of the low-mass companion in the CV SDSS 103533.03+055158.4 (SDSS 1035 for short).

The orbital period of SDSS 1035 is only 82 min, so small features such as the white dwarf are eclipsed in less than a minute. To accurately measure these rapid changes of brightness in such a faint star, they used ULTRACAM, an instrument that uses CCDs to measure the brightness of CVs and other rapidly varying stars. The data quality is impressive and leads to a mass for the companion accurate to about 4%. This is good enough to show convincingly that they were observing a genuine dead CV because the companion is well below the limit of 0.072 solar masses, after which a star cannot sustain nuclear reactions in its core. Objects that are born with masses below this limit are known as brown dwarfs.

A typical CV is smaller than the Sun, so there is a good chance that the orientation of the binary is such that the companion eclipses the white dwarf once every orbit as seen from Earth. This will lead to an apparent dimming of the CV every orbit during the few minutes that the companion blocks the light from the white dwarf. SDSS 1035 is an eclipsing CV, so there is a wealth of information to be gleaned from the changes in brightness during the eclipse. These show, for example, that the mass transferred from the low-mass companion forms a disc around the white dwarf with a bright spot on its outer edge due to the inflowing material.

A GASEOUS METAL DISK AROUND A WHITE DWARF

As the main-sequence stars hosting planetary systems evolve through the red-giant stage, they swell up and destroy planets and asteroids out to many hundred solar radii. However, a team of astronomers found a metal-rich gas disk around a moderately hot and young white dwarf.

The mass of the white dwarf implies a relatively massive main-sequence progenitor of ~4 to 5 solar masses, which will have expanded to a radius of ~1000 solar radii. It is therefore impossible that the material making up the present-day disk has survived the giant phase at its current location; it must instead have been brought inward from outside a distance of 1000 solar radii.

The white dwarf SDSS J122859.93+104032.9 (henceforth SDSS 1228+1040) was identified as a moderately hot 0.77 solar-mass white dwarf, but noted very unusual emission lines from the Ca II 850- to 866-nm triplet, as well as weaker emission lines from Fe II at 502 and 517 nm. The line profiles of the Ca II triplet display a distinct double-peaked morphology, which is the hallmark of a gaseous, rotating disk. Time-resolved spectroscopy and photometry do not reveal any radial velocity or brightness variations. These data exclude the possibility that SDSS 1228+1040 is an interacting white dwarf binary, in which an accretion disk around the white dwarf forms from material supplied by a nearby companion star. Furthermore, the absence of Balmer and helium emission lines implies that the gaseous disk around SDSS 1228+1040 must be extremely deficient in volatile elements, which independently rules out an interacting binary nature for this object.

A dynamical model of the double-peaked emission lines constrains the outer disk radius to just 1.2 solar radii. A possible origin of such dust disks is the tidal disruption of either comets or asteroids. Asteroids appear to be more likely candidates because they can explain the large amount of metals accreted by the white dwarfs from the dusty environment, as well as the absence of hydrogen or helium. Furthermore, the radius derived from the

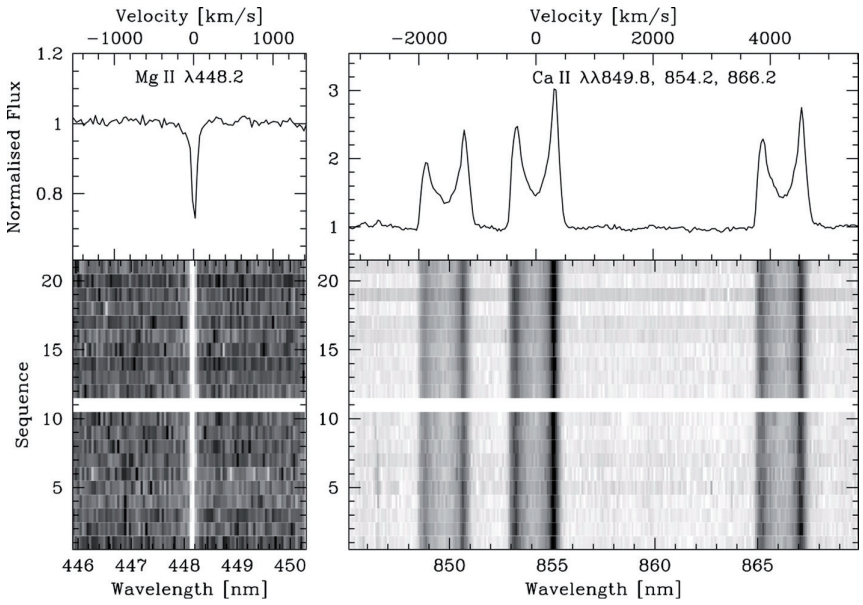

Figure 7. Time-resolved spectroscopy of SDSS 1228+1040. Medium-resolution spectroscopy of SDSS 1228+1040 was obtained with the double-arm spectrograph ISIS on the WHT. Two sets of 10 consecutive spectra each were obtained. The bottom panels show the two time series of spectra, each extending over 1.7 hours, centered on the calcium emission triplet (right) and the magnesium absorption line (left). The normalised average spectra are shown in the top panels. Radial velocities are given in the upper axes with respect to CaII 854 nm (right) and MgII 448 nm (left). The radial velocity of the MgII line is stable to within ±4 km/s over time scales of 20 min to 1 day. Additional time-series photometry obtained with the Wide-Field Camera at the INT shows the star at constant brightness within ±0.01 mag (figure from Gänsicke et al., 2006, Science, 314, 1908. Reprinted with permission from AAAS).

dynamical model is compatible with the tidal disruption radius for a rocky asteroid.

Although the detection of asteroid debris around SDSS 1228+1040 represents a possible link to the existence of planetary systems around their main-sequence progenitor stars, modelling the excess infrared luminosity provides no direct information on the geometric location and extension of the dust, impeding a more detailed understanding of the nature and origin of the circumstellar material.

But certainly the infrared excess found around metal-polluted white dwarfs hotter than 15,000 K suggests that the radiation field of these hot white dwarfs causes sublimation of a dust disk and the case of SDSS 1228+1040 demonstrates that planetary debris material can be detected around younger and hotter white dwarfs in the form of gaseous disks. Furthermore, the detection of a metal-rich debris disk around this relatively massive white dwarf indicates that the formation of planetary systems can take place also around short-lived massive stars.

THE LEAST-MASSIVE BROWN DWARFS IN THE PLEIADES

A search for low-mass brown dwarfs in the Pleiades open cluster has led to the identification of the least massive cluster members: BRB 28 and 29 have masses of the order of 25 Jupiter masses, and they were confirmed as cluster members from HK_S photometry and proper motion measurements using the Long-slit Intermediate Resolution Infrared Spectrograph (LIRIS) on the WHT.

This discovery will help to constrain evolutionary models for L-type brown dwarfs and to extend the study of the cluster mass function to lower masses. The existence of such low-massive brown dwarfs and their frequency in relation to higher mass stars might indicate the presence of planetary-mass bodies floating freely in the Pleiades.

FIRST DETECTION OF RUBIDIUM IN ASYMPTOTIC GIANT BRANCH STARS

A long debated issue concerning the nucleosynthesis of neutron-rich elements in Asymptotic Giant Branch (AGB) stars is the identification of the neutron source. Low- and intermediate-mass stars (1 to 8 solar masses) evolve towards the asymptotic giant branch (AGB) phase after the completion of hydrogen and helium burning in their cores, before they form planetary nebulae, ending their lives as white dwarfs. Basically, an AGB star is composed of an inert carbon-oxygen (C-O) core surrounded by a He-rich intershell and an extended H-rich convective envelope. Nuclear energy release is dominated by the H shell and interrupted periodically by thermonuclear runaway He-shell "thermal pulses" that initiate a series of convective and other mixing events. Strong mass loss enriches the interstellar medium (ISM) with the products of the resulting complex nucleosynthesis. During this thermally pulsing AGB (TP-AGB) phase, stars originally born O-rich (reflecting the ISM composition) can turn C-rich (C/O>1) as a consequence of the "dredge-up" of processed material from the bottom of the convective envelope to the stellar surface.

Mixing of protons into the He-rich intershell during the TP-AGB phase leads to reaction chains producing free

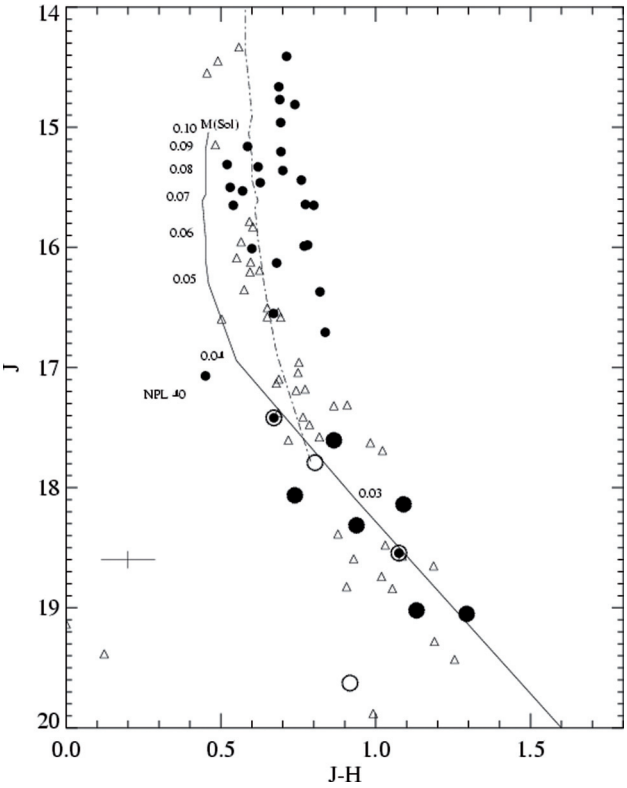

Figure 8. J versus J-H colour-magnitude diagram for all Pleiades very low-mass star and brown dwarf candidates of the survey with lithium abundance or proper motion consistent with membership (filled circles) (figure from Bihain et al., 2006, A&A, 458, 805).

neutrons, which allow production of neutron-rich elements such as Rb, Sr, Y, Zr, Ba, La, Nd, and Tc by slow neutron capture on iron nuclei and other heavy elements (the s process). There are two possible chains for the neutron production: $^{13}C(\alpha,n)^{16}O$ and $^{22}Ne(\alpha,n)^{25}Mg$. The ^{13}C neutron source operates at relatively low neutron densities and temperatures in TP-AGB stars during the inter pulse period. The ^{22}Ne neutron source operates at much higher neutron densities and requires higher temperatures, which are achieved only while the convective thermal pulse is ongoing.

In the more massive AGB stars where these high temperatures are more easily achieved, the s-process elements are expected to form mainly through the ^{22}Ne reaction that also strongly favours the production of the stable isotope ^{87}Rb (because of the operation of a branching in the s-process path at ^{85}Kr that modifies the isotopic mix between ^{85}Rb and ^{87}Rb).

Unfortunately, the Rb isotope ratio cannot be measured in stellar sources even with the help of very-high-resolution spectra, because the lines are too broad, and thus it is difficult to use this parameter as a neutron density

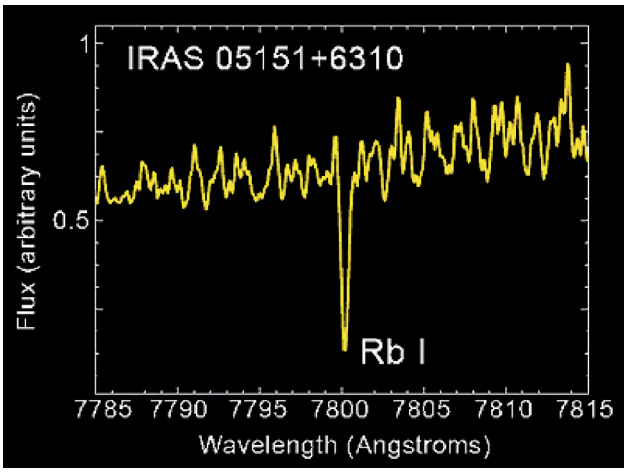

Figure 9. Rubidium line at 7800Å as detected by the UES spectrograph on the WHT in BW Cam, one of the AGB stars observed in this study. Credit: IAC/ESA.

indicator. As an alternative, the total Rb abundance can be used. The theoretical prediction is that the relative abundance of Rb to other nearby elements produced by the s-process, such as Zr, Y, and Sr, is a powerful indicator of the neutron density at the s-process site and, as such, is a good discriminator of the operation of the ^{13}C versus the ^{22}Ne neutron source in AGB stars.

A team of astronomers using the Utrecht Echelle Spectrograph (UES) on the WHT reported for the first time intermediate-mass (4 to 8 solar masses) AGB stars in our Galaxy that are Rb-rich as a result of overproduction of the long-lived radioactive isotope ^{87}Rb. This represents direct observational evidence, predicted theoretically 40 years ago, that the slow-neutron capture process following the $^{22}Ne(\alpha,n)^{25}Mg$ reaction must be the dominant neutron source in these stars.

Because huge amounts of Rb-rich processed material can be transferred to the interstellar medium by massive AGB stars, this result has also relevant implications for the Rb primeval solar nebula abundance.

Radioactive dating studies of primitive chondrites assume that the initial conditions are known and that the oldest components of chondrites evolved without external exchange of Rb. The results of this research, however, suggests that the initial abundance may have been altered by a nearby population of massive AGB stars during the early evolution of our Solar System, and consequently, the Rb abundance measured in primitive meteorites should be considered only as a qualitative measure of antiquity.

THE MEDIUM-RESOLUTION INT LIBRARY OF EMPIRICAL SPECTRA

A project aimed at improving the existing tools for extracting stellar population information using the optical region of composite spectra was started by a team of astronomers mainly using the IDS spectrograph on the INT. Although the main motivation of this work was to use this new calibration to study the stellar content of galaxies using spectra of unresolved stellar populations, it was anticipated that the material could also be useful in other areas of astronomy.

This included a new stellar library (MILES – the Medium-resolution Isaac Newton telescope Library of Empirical Spectra), a set of homogeneous atmospheric parameters, a redefinition and recalibration of spectral-line indices, empirical fitting functions describing the behaviour of indices with stellar parameters, and stellar population model predictions.

A comprehensive spectral library with medium-to-high resolution and a good coverage of the Hertzsprung–Russell (HR) diagram is an essential tool in several areas of astronomy. In particular, this is one of the most important ingredients of stellar population synthesis, providing the behaviour of individual stellar spectra as a function of temperature, gravity and chemical abundances.

Unfortunately, the empirical libraries included in this kind of models up to now, contained few stars with non-solar metallicity, compromising the accuracy of predictions at low and high metallicity. This problem has usually been partially solved by using empirical fitting functions, polynomials that relate the stellar atmospheric parameters (T_{eff}, log g, and [Fe/H]) to measured equivalent widths. These functions allow the inclusion of any star required by the model (but within the stellar atmospheric parameter ranges covered by the functions), using a smooth interpolation.

However, the new generation of stellar population models go beyond the prediction of individual features for a simple stellar population, and they attempt to synthesise full spectral energy distributions (SEDs). In this case, the fitting functions cannot be used, and a library of stars covering the full range of atmospheric parameters in an ample and homogeneous way was urgently demanded. Moreover, although the evolutionary synthesis codes do not require absolute fluxes, the different stellar spectra must be properly flux calibrated in a relative sense so that the whole SED can be modelled. This, however, is quite difficult to achieve in practice, due to the wavelength-dependent flux losses caused by differential refraction when a narrow slit is used in order to obtain a fair spectral resolution.

Another important caveat in the interpretation of the composite spectrum of a given galaxy is the difficulty of disentangling the effects of age and metallicity. Due to blending effects, this problem is worsened when working at low spectral resolution, as is the case when low-resolution stellar libraries are used. There are a few studies that have attempted to include spectral features at higher resolution. However, predicting such high-dispersion SEDs is very difficult owing to the unavailability of a library with the required input spectra.

Whilst the new generation of large telescopes are already gathering high-quality spectra for low- and high-redshift galaxies, the stellar population models suffer from a lack of extensive empirical stellar libraries to successfully interpret the observational data. At the moment, the available stellar libraries have important shortcomings, such as a small number of stars, poor coverage of atmospheric parameters, narrow spectral ranges, low-resolution and non-flux-calibrated response curves.

The MILES library overcomes some of the limitations of the previous libraries. The new library covers the spectral range 3525–7500 Å at spectral resolution of 2.3 Å [full width at half-maximum (FWHM)]. The spectra of 985 stars with metallicities ranging from [Fe/H]~ –2.7 to +1.0 and a wide range of temperatures were obtained using the IDS spectrograph on the INT over a total of 25 nights in 5 different runs.

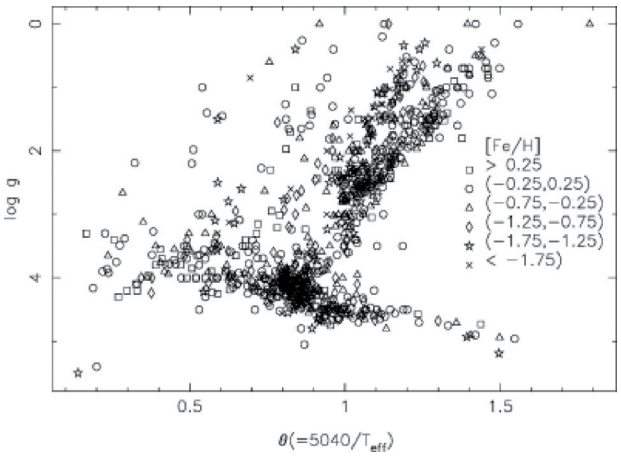

Figure 10. Gravity–temperature diagram for the library stars. Different symbols are used to indicate stars of different metallicities, as shown in the key (figure from Sánchez-Blázquez et al., 2006, MNRAS, 371, 703).

SHORT TIME-SCALE VARIABILITY IN THE FAINT SKY VARIABILITY SURVEY

There is a wide range of photometrically variable systems in the Universe. The range of time-scales on which these systems vary, is as wide as the physical processes that produce their variability. For example, we have intrinsically variable stars, where the variability is caused by changes in their internal structure or atmospheres that vary with time-scales of minutes to years. Other stars show variability because they rotate and their surface is inhomogeneous, for example, because of star spots, or because they form part of a binary or multiple system and their revolution around the centre of mass of the system results in changes in the detected flux due to the changing aspect of a non-isotropically emitting surface or eclipses.

This is also the case for planets orbiting stars. The time-scale of the variability in this case is dictated by the orbital parameters of the system and can range from seconds to years. Near-earth objects (NEOs), such as asteroids, also show variability as they rotate and are non-spherical.

We find photometric variability in extragalactic objects as well, such as quasars, where the variability is probably the result of material being accreted by the central engine, or 'one off' systems, such as gamma-ray bursts (GRBs) or supernovae (SNe) where the variability is produced by intrinsic changes in the structure of an astronomical object that take place only once.

The study of variability provides important information about the physical nature of the variable objects, leads to the discovery of new classes of objects, helps to study the physical structure of stars, for example, pulsating stars, allows us to obtain information on Galactic structure through the use of variables such as RR Lyrae as standard candles, and is the key to determining extragalactic distances through the use of standard candles, such as Cepheids and Type Ia SNe.

Most of our knowledge of variability is based on the study of apparently bright sources, which naturally selects members of intrinsically bright populations. At present, little is known about variability of intrinsically fainter populations, because in bright samples they are lacking altogether or are only represented by a few members.

The Faint Sky Variability Survey (FSVS) was one of the programmes of the INT Wide Field Survey and it was designed to account for this deficit by studying two unexplored regions of the variability space: the short time-scale variability region (down to tens of minutes) and the intrinsically faint variable sources (down to V = 24 mag) at mid and high Galactic latitudes. The FSVS also contains colour information for all targets, giving us the option of positioning objects in the colour–colour diagram, as well as finding the variability time-scales and amplitudes that characterise them. The main aims of the FSVS are thus to obtain a map of a region of the Galaxy (~21 deg^2) in variability and colour space, to determine the population density of the different variable objects that reside in the Galaxy and to find the photometric signature of up-to-now unknown intrinsically faint variable populations.

The full FSVS data set consists of 78 Wide Field Camera (WFC) fields, covering an area in the sky located at mid and high Galactic latitudes ($-40 < b < -21$, $15 < b < 50$, $89 < b < 90$). For each field, they took one set of B-, I- and V-band observations on a given photometric night. Photometric variability observations were taken with the V filter on several consecutive nights. On average, fields were observed 10–20 times within one week in the V band. Exposure times were 10 min with a dead time between observations of 2 min. This observing pattern allows one to sample periodicity time-scales from 2×(observing time+dead time) (i.e. 24 minutes) to twice the maximum time-separation of observations (which ranges from 3 to 13 days). All fields were re-observed years later to determine proper motions.

A V-band variability analysis of the point sources in the FSVS on time-scales from 24 min to tens of days showed that about one per cent of the point sources down to V = 24 are variables. Of these, about 50 per cent show variability time-scales shorter than 6 h, 22 per cent show variabilities between 6 h and 1 d, 20 per cent between 1 and 4 d and 8 per cent show periods longer than 4 d. The total number of variables is dominated by main sequence sources. The distribution of variables with spectral type is fairly constant along the main sequence, with 1 per cent of the sources being variable, except between spectral types F0 and F5, where the fraction of variable sources increases to about 2 per cent. For bluer sources, above the main sequence, beyond the blue cut-off at $(B-V)<0.38$, this percentage increases to about 3.5. About a third of the total number of short time-scale variables found in the survey were not detected in either B or/and I band. These show a similar variability time-scale distribution to that found for the variables detected in all three bands.

The observed variability is likely to be the result of pulsations, binarity and stellar rotation as well as intrinsic flaring activity in the case of main sequence stars. One RR

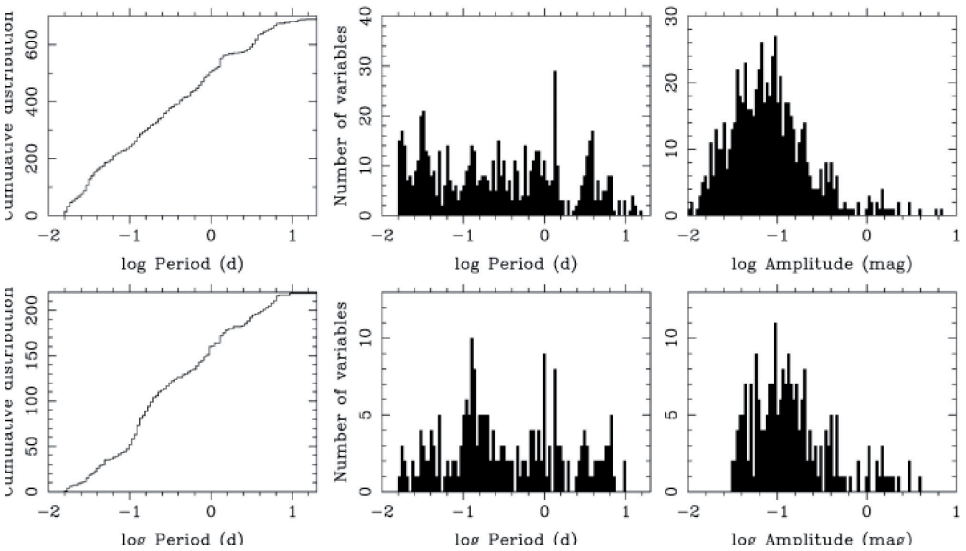

Figure 11. Histograms showing the cumulative period distribution (left hand panels), the period distribution (middle panels) and the amplitude distribution (right-hand panels) for the short-term variable point sources in the FSVS. Top panels: the 689 out of 744 sources with accuracies in the periods and amplitudes of the order of 30 per cent or less. Bottom panels: sources where the error in their periods and amplitudes is of the order of 10 per cent or less (figure from Morales-Rueda, 2006, MNRAS, 371, 1681).

Lyr candidate found is the furthest known in the Galaxy and could allow the determination of the mass of the Milky Way.

The highest space densities of variables found in the FSVS (i.e.17 deg^{-2}) show periods below 12 h. These include CVs, RR Lyr stars, and other short-period pulsators, such as δ Scuti stars. They find a density of four variables per deg^2 centred on a 1 d period which includes longer-period CVs, RR Lyr and other pulsators, like γ Doradus stars and Population II Cepheids. A space density of two variables per deg^2 at 3.75 d includes some longer-period CVs, γ Doradus stars, Population II Cepheids and longer-period pulsators, such as subdwarf B stars. At 12.75 d, they also find two variables per deg^2. These would be mainly binaries with those orbital periods and Population II Cepheids.

The FSVS is complete down to *V*=22 for CVs in the minimum period (80 min), as long as they show variability amplitudes of the order of 0.4 mag. It is complete down to *V*=22 for periods between 80 min and 1 d in a 17.82-deg^2 area of the survey, as long as the amplitude of the variability is at least 0.7 mag. This includes most RR Lyr stars.

NEW PLANETARY NEBULAE DISCOVERED BY IPHAS

The INT/WFC Photometric Hα Survey of the Northern Galactic Plane (IPHAS) is currently mapping 1800 degrees^2 of the Northern Galactic plane (a band between b= –5 to +5 degrees) in three filters using the INT Wide Field Camera. The survey is an international collaboration of 15 institutes. A narrow-band Hα and two Sloan filters (r' and i') are used for matched 120, 30, and 10 s exposures, respectively, spanning the magnitude range r'=13 to 20 mag for point sources. IPHAS is the first fully-photometric Hα survey of the Galactic plane. It will discover around 40,000 new emission-line stars, including young stars (T Tau, Herbig AeBe stars, etc.), evolved stars (post-AGB, LBVs, etc.) as well as binaries (CVs, symbiotic stars, etc.) in addition to thousands of extended nebulae such as Planetary Nebulae (PNe), H-H objects, HII regions, SN remnants, etc.

Two systematic searches for PNe are currently conducted on the IPHAS data. Extended PNe are searched visually from continuum subtracted mosaics of IPHAS data while the compact PNe search is based on IPHAS catalogue information. The first step to select compact PN candidates is to filter out all objects which are too close to the borders of the CCDs or to the areas of bad pixels, as well as sources which are not classified as stars or extended objects. Also a first cut in the r'–Hα plane is made removing all objects with r'–Hα < $(r'–H\alpha)_{median}$ + 1, which removes the majority of the stellar locus objects. They also remove sources where the positional match between individual images is worse than 0.65 arcsec. Together with the visual search for extended PNe they expect to find a total of 500–1000 new Galactic PNe.

The discovery of the first new PN from this survey is an unusual object located at a large galactocentric distance and has a very low oxygen abundance. The so-called "Príncipes de Asturias" nebula shows an intricate morphology: there is an inner ring surrounding the central star, bright inner lobes with an enhanced waist, and very faint lobular extensions reaching up to more than 100".

Another example is the Ear Nebula shown in Figure 13. The exposure times amounted to 50 minutes in Hα and 30

Figure 12. The "Príncipes de Asturias" nebula or IPHAS PN-1. Credit: Antonio Mampaso, Romano Corradi and the IPHAS Collaboration.

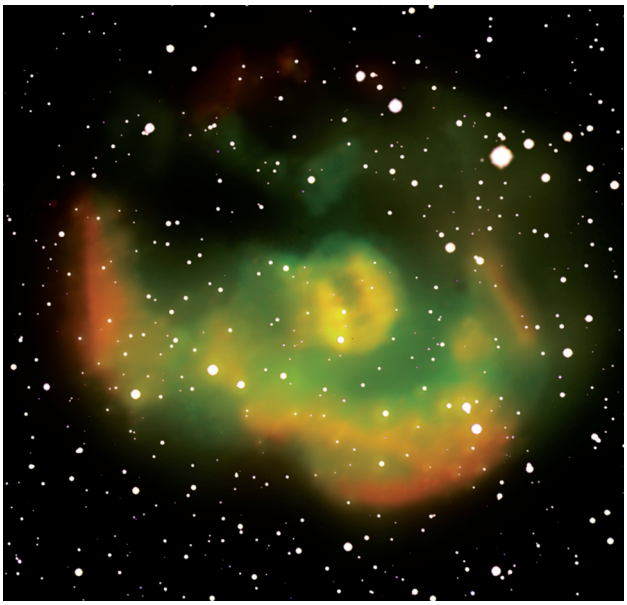

Figure 13. The Ear Nebula is one of the new PNe discovered by IPHAS. This is a two-colour image, red for Hα and green for [O III]. North is to the right and East is to the top. Credit: Laurence Sabin, Nick Wright and the IPHAS Collaboration.

minutes in [O III]. The nebula was confirmed to be a relatively old planetary nebula using the ISIS spectrograph on the William Herschel Telescope.

A WHIRLPOOL IN THE WAKE LEFT BY A DYING STAR

The central star of Sharpless 2-188 is 850 light years away and it is travelling at 125 kilometres per second across the sky. Observations show a strong brightening in the direction in which the star is moving and faint material stretching away in the opposite direction.

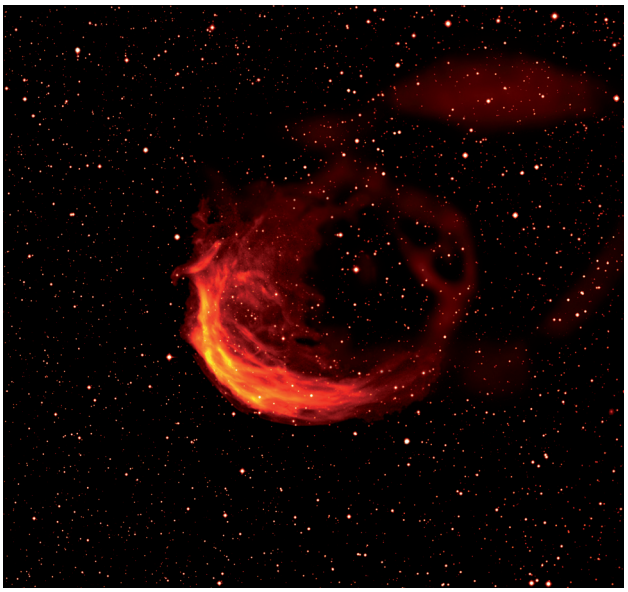

Figure 14. A combined image showing the bright regions and the faint regions behind the bright arc of the Sharpless 2-188 nebula (figure from Wareing et al., 2006, MNRAS, 366, 387).

The astronomers compared the predictions from a simulation in three-dimensions of the movement of a dying star through surrounding interstellar gas with observations of the planetary nebula Sharpless 2-188 taken as part of the IPHAS survey. They believe that the bright structures in the arc observed ahead of Sharpless 2-188 are the bowshock instabilities revealed in the simulations, which will form whirlpools as they spiral past the star downstream to the tail.

IPHAS INITIAL DATA RELEASE

The IPHAS collaboration, together with the Cambridge Astronomical Survey Unit (CASU) and the Astrogrid Virtual Observatory (VO) announced the availability of the IPHAS Initial Data Release (IDR).

The IPHAS IDR is a photometric catalogue of more than 200 million objects coupled with associated imaging data covering about 1700 square degrees in three colours. The survey is aimed at revealing large scale structure in our local galaxy, and also the properties of key early and late populations making up the Milky Way.

The object catalogues and data quality control parameters have been ingested in a Sybase Relational Database Management System. The access to the primary data products has been implemented through use of standard VO publishing interfaces as provided by the Astrogrid system.

BROWN DWARFS AND ISOLATED PLANETARY-MASS OBJECTS

Using data from a deep infrared survey of the young σ Orionis open cluster, astronomers searched for low-mass objects in the central region down to 6 Jupiter masses and studied their mass distribution.

The survey was built from data taken with the Wide Field Camera on the INT and ISAAC on VLT's UT1 Antu. Deep *I*- and *J*-band images of a 0.22deg^2 region close to the cluster centre were obtained, reaching limiting magnitudes of *I*~24.1 and *J*~21.8 respectively. The LIRIS infrared spectrograph and imager on the WHT was also used to obtain some deep images in the *H* and K_s bands. And follow-up of candidates was performed using data from the 2MASS survey, the Spitzer Space Telescope, and other telescopes.

The survey yielded 30 very young cluster low-mass objects, among them brown dwarfs (BDs) and isolated planetary-mass objects (IPMOs). By studying their mass spectrum, or counting the number of objects per mass interval, the astronomers found a rising mass spectrum in the mass interval 0.11 to 0.006 solar masses implying that IPMOs could be as frequent as our Sun.

They found no direct evidence for the presence of an opacity-mass limit for objects formed via fragmentation and collapse of molecular clouds implying that BDs and IPMOs probably form as an extension of the low-mass star formation process. Any possible mass cut-off would lie below 0.006 solar masses or 6 Jupiter masses.

Another interesting result of their research is that almost half of the studied BDs harbour protoplanetary discs.

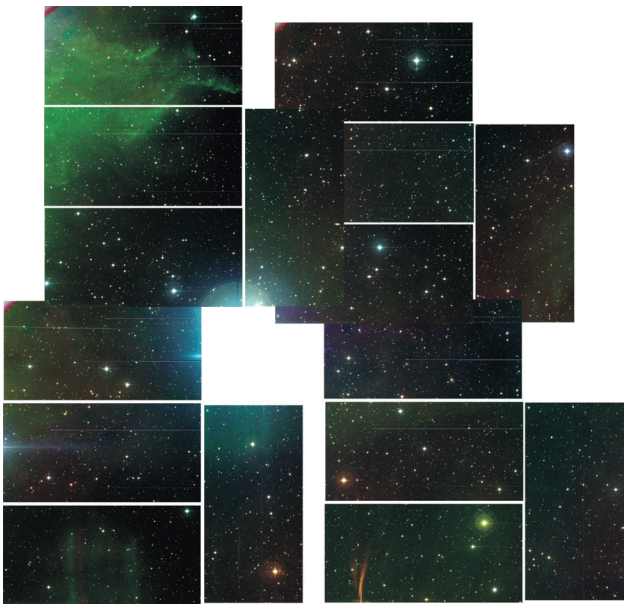

Figure 15. Colour composition of the σ Orionis open cluster (North is up and East to the left) from images taken using the Wide Field Camera on the INT.

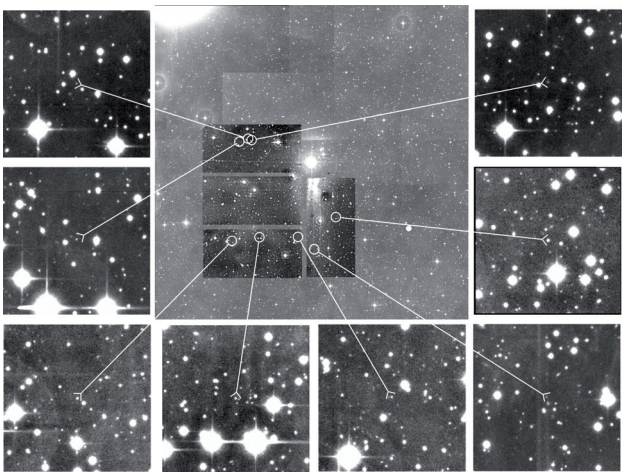

Figure 16. Mosaic of I-band images centred on σ Orionis taken with the Wide Field Camera on the INT showing the location of some of the low-mass objects. North is up and East to the left. The size of each Wide Field Camera frame is about 11×22 arcmin^2. The background image is from DSS-2-IR.

A LOW-MASS PRE-MAIN-SEQUENCE ECLIPSING BINARY SYSTEM

Eclipsing binaries are a special class of spectroscopic binaries, systems where the components are so close together that they cannot be separated by imaging. In an eclipsing binary, the system is edge-on as seen from the Earth, so one star passes in front of the other every half orbit, causing the total light emitted to dim in a periodic fashion. By measuring the shape of these eclipses in a light curve of the system, astronomers can derive the radii of the stars in the binary.

The binary system JW 380, located in the very young Orion Nebula Cluster (ONC), was identified using time-series imaging observations taken with the Wide Field Camera on the INT. These observations were part of the Monitor project, a large-scale survey searching for eclipsing binary and transiting extrasolar planet systems in a number of young open star clusters.

Follow-up spectroscopic observations obtained using the FLAMES fibre-fed spectrograph on the VLT UT2 and the NOAO Phoenix spectrograph on Gemini-South were used to derive the radial velocities and hence component masses of the stars, as well as to confirm the system's membership in the ONC.

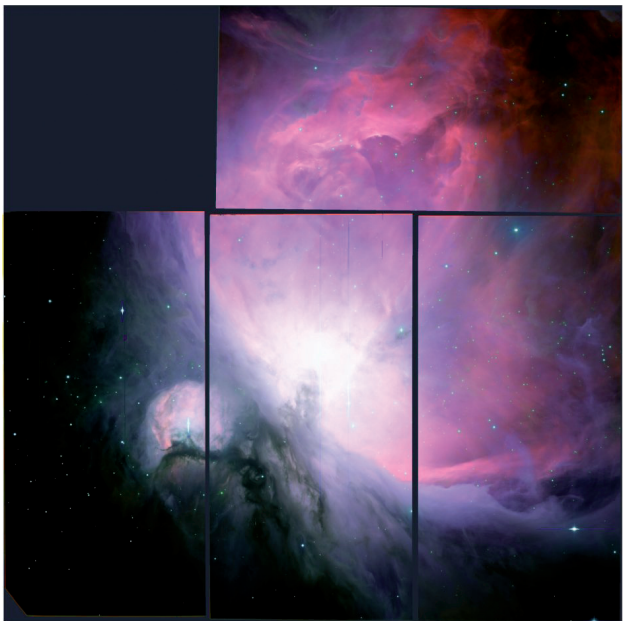

Figure 17. Colour composition of a Wide Field Camera image of the Orion Nebula. Credit: Jonathan Irwin.

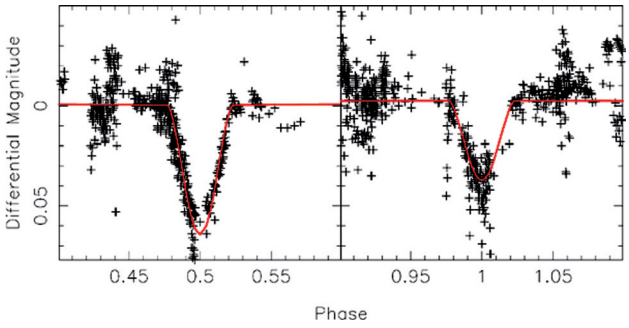

Figure 18. Eclipses in the light curve of JW 380 (figure from Irwin et al., 2007, MNRAS, 380, 54).

From these data, the astronomers were able to obtain accurate empirical measurements of both the masses and the radii of the component stars of JW 380. The star system comprises of a pair of 0.26, 0.15 solar-mass pre main sequence stars, with measured radii of 1.2 and 0.9 solar radii respectively.

This is the second eclipsing binary identified in the ONC. The first was announced during 2006 and contains two brown dwarfs, or "failed stars", systems which are too cool to burn hydrogen into helium. JW 380 contains instead two M-dwarf stars of 3-4 times heavier mass. By identifying eclipsing binaries spanning a range of masses and ages, it is possible to map the evolution of stellar radius with age empirically, which can then be compared to models of stellar evolution to help understand how stars evolve.

The observations confirm the predictions of theoretical models that low-mass stars are "bloated" at these extremely young ages because they are still contracting in the stages between birth and arrival onto the main sequence. Comparing the measured radii with the model predictions indicates an age of 2-3 Myrs, consistent with existing estimates for the ONC.

A third component in the system is also visible in the spectroscopic observations. This may be physically associated with the binary, making a triple star system with the third component in a wide orbit. This will be the subject of future follow-up observations to derive its orbital parameters.

The present result is part of the Monitor Project, a large-scale photometric survey of nearby open clusters and star-forming regions, aiming to measure time-series photometry for >10,000 cluster members over >10 deg^2 of sky, to find low-mass eclipsing binary and planet systems. Peak rms accuracy over the entire data set is better than ~2 mmag using aperture photometry, with rms <1 per cent over ~4 mag, in data from 2- and 4-m class telescopes with wide-field mosaic cameras, among them, the INT Wide Field Camera.

A STRONGLY-IRRADIATED TRANSITING GAS-GIANT EXOPLANET

The SuperWASP cameras are wide-field imaging systems sited at the Observatorio del Roque de los Muchachos and the Sutherland Station of the South African Astronomical Observatory. Each instrument has a field of view of some ~482 square degrees with an angular scale of 13.7 arcsec per pixel, and is capable of delivering photometry with accuracy better than 1% for objects having *V*~7.0–11.5. The systems, while designed to monitor fields with high cadence, are capable of surveying the entire visible sky every 40 minutes. Depending on the observational strategy, the data rate can be up to 100 Gb per night. A robust, largely automatic reduction pipeline and advanced archive is used to serve data products to the Wide Area Search for Planets (WASP) consortium members. The Isaac Newton Group of Telescopes is a member of the WASP consortium and the design of the SuperWASP cameras was inspired by the early success of the CoCAM series of cameras designed and built at the ING from 1996 to 1998, one of which was responsible for the discovery of the so-called Sodium Tail in Comet Hale-Bopp 1995.

The first planets discovered by SuperWASP were WASP-1b and WASP-2b in 2006. WASP-1b was named as "Garafía-1" after the name of the municipality that hosts the Observatorio del Roque de los Muchachos, and both were

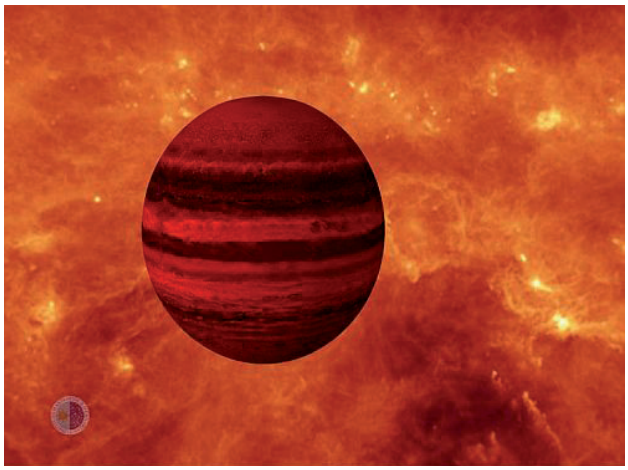

Figure 19. Top: SuperWASP-N cameras at the Observatorio del Roque de los Muchachos. Credit: David Anderson. Bottom: WASP-3b is one of hottest extrasolar planets ever detected. Credit: artist impression by IAC's multimedia service.

actually the first ever exoplanets discovered at the observatory.

Following this success, the WASP and SOPHIE collaboration announced the discovery of three more exoplanets: WASP-3b, WASP-4b and WASP-5b. WASP-3b was one of the hottest exoplanets discovered until then. At a temperature of more than 1700 degrees Celsius, WASP-3b has the potential to place stringent constraints on exoplanet atmospheric models. The discovery of the three transiting planets was named 'the 6th most important scientific discovery of 2007' in Time Magazine's Top Ten List.

The first transits of WASP-3b were detected by the SuperWASP cameras and they were then confirmed by the IAC80 telescope at the Observatorio del Teide, Tenerife, as part of the Canarian Observatories' International Time Programme for 2007, and by the University of Keele's 60-cm telescope. The discovery confirmation, using the radial velocity method, came from data obtained with the SOPHIE spectrograph on the Observatoire de Haute Provence's 1.93m telescope.

Observations made with the adaptive-optics system NAOMI+INGRID on the WHT were used to exclude the possibility of a nearby eclipsing-binary system being the cause of the transits. WASP-3, the host star, lies at approximately 220 parsecs or 720 light years and no companion stars were found to lie within 45 astronomical units of WASP-3.

THE AXISYMMETRIC WIND OF THE POST RED SUPERGIANT IRC +10420

IRC +10420 is an extremely luminous star that inhabits the so-called yellow void on the HR diagram between the red and blue supergiants. There is considerable evidence that the star is evolving rapidly away from the red supergiant (RSG) phase toward the luminous blue variable (LBV) or Wolf-Rayet (W-R) phases. As such, this object represents a potential link between the key post-main-sequence mass-losing stages and is therefore considered extremely important for the study of massive stellar evolution.

The star has been observed to gradually increase in temperature from ~6000 to ~9200 K in the last 30 years and the material the star has recently ejected may be the precursor to a LBV/W-R nebula. These nebulae are often axisymmetric, but it is unclear how these nebulae are formed. Hydrodynamic studies have shown that axisymmetric morphologies can arise from either an axisymmetric wind in the LBV/W-R phase, or a spherically symmetric wind blowing into a slower axisymmetric wind ejected in the RSG phase. As wind axisymmetry may be linked to rotation, which itself plays an important role in the evolution of a massive star, and as IRC +10420 appears to be somewhere between the LBV/W-R and RSG phases, determining the true geometry of the star's present-day wind may provide insight into the formation mechanism of the bipolar nebulae of massive stars. Furthermore, it may also provide clues as to the role of rotation in its

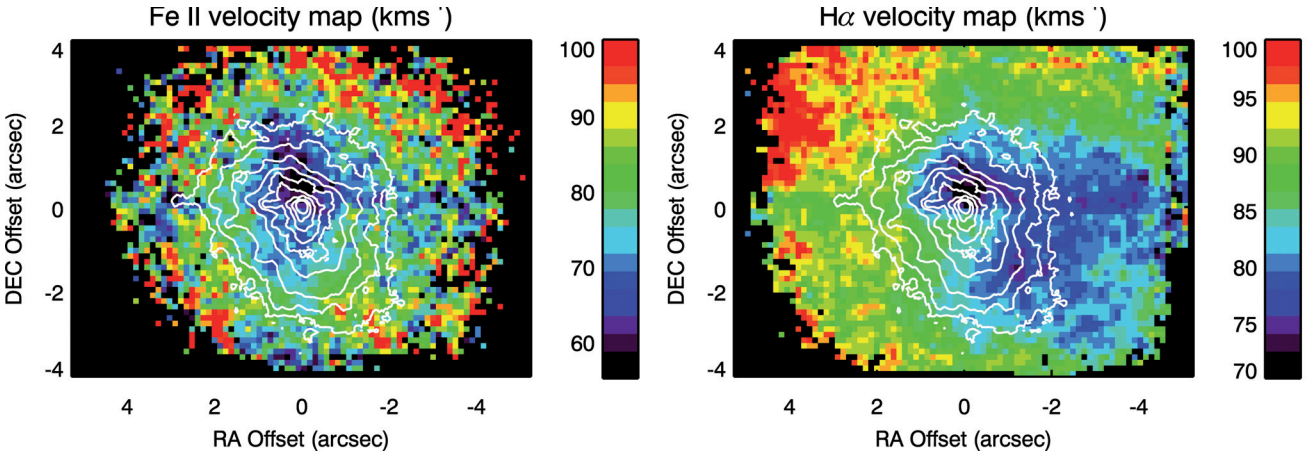

Figure 20. Velocity maps, as determined from Gaussian fits to the emission lines. The images are overlayed with a contour map of the B-band HST image. Images are heliocentric corrected, and colour bars to the right of each plot show the velocity scale. The two maps show different behaviour: the Fe II map shows lower velocities in the centre and higher velocities in the outer regions; while the Hα map shows the lowest velocities in the southwest and the highest in the northeast. (Extracted from Davies et al., 2007, ApJ, 671, 2059).

subsequent evolution and the connection to other classes of massive star.

The geometry of IRC +10420's wind has been the topic of much discussion over the last ~20 years, yet a consensus remains elusive due to contradictory evidence. The confusion was complete when astronomers using HST long-slit spectroscopy, utilised the star's reflection nebula as a tool with which to view the Hα emission from different angles. With the slit aligned along the long axis of the nebula, they showed that the velocities of the two peaks in their H alpha profile were uniform. This was inconsistent with a circumstellar disk or a bipolar outflow, and led to the conclusion that the star showed no evidence of axisymmetry in the present-day wind. However, they only observed two slit positions, each roughly parallel to the long axis of the nebula and separated by 0.5 arcsec.

With integral-field spectroscopy using NAOMI+OASIS on the WHT, another team of astronomers improved on the data with spatially resolved spectroscopy across the whole of the inner nebula. To investigate the present-day mass-loss geometry of the star, they studied the appearance of the line emission from the inner wind as viewed when reflected off the surrounding nebula and they found that, contrary to previous work, there is strong evidence for wind axisymmetry, based on the equivalent width and velocity variations of the H alpha and Fe II 6516Å lines. They attribute this behaviour to the appearance of the complex line profiles when viewed from different angles and they also speculate that the Ti II emission originates in the outer nebula in a region analogous to the Sr filament of η Carinae, based on the morphology of the line emission. Finally, they suggest that the present-day axisymmetric wind of IRC +10420, combined with its continued blue-

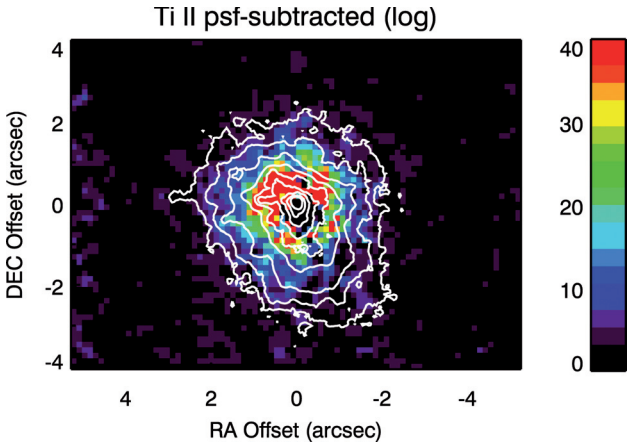

Figure 21. Continuum-subtracted, PSF-subtracted image of IRC +10420 in the light of Ti II, scaled in units of σ above the sky background. The image is overlayed with a contour map of the B-band HST image. Contrary to similar maps of the Hα and Fe II emission, the Ti II emission does not trace the morphology of the reflection nebula (figure from Davies et al., 2007, ApJ, 671, 2059).

ward evolution, is evidence that the star is evolving toward the B[e] supergiant phase.

THE MILLENNIUM GALAXY CATALOGUE

The Millennium Galaxy Catalogue (MGC) is a survey of over ten thousand giant galaxies, each comprising of up to 10 billion stars as well as bulges, discs and super-massive black holes. The imaging data were obtained using the Wide Field Camera on the INT. The survey was able to determine how much of the Universe's matter is locked away in black holes, some of which are one million billion times more massive than the Earth. By adding up each key component it is found that the Universe has used about twenty percent of its original fuel reserves.

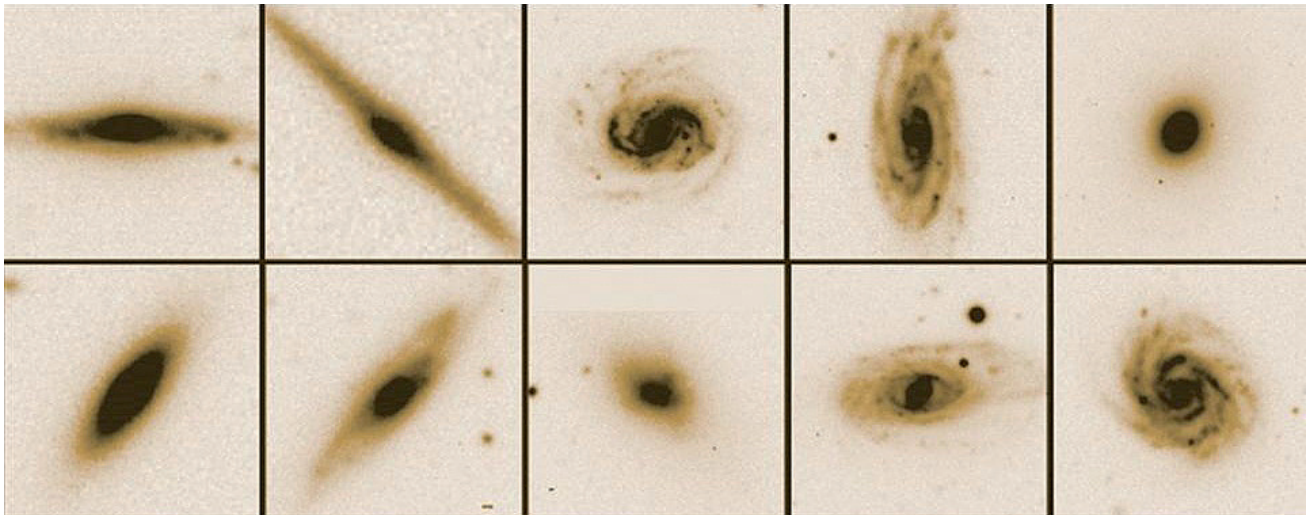

Figure 22. Sample images from the Millennium Galaxy Catalogue (figure from Driver et al., 2007, MNRAS, 368, 414).

Tracking down what happened to normal matter dating back to the Big Bang 14 billion years ago has remained one of the most important goals for cosmologists for many years. The new survey reveals that about 20% is locked up in stars, a further 0.1% lies in dust expelled from the massive stars (and from which solid structures like the Earth and man are made), and about 0.01% is in the form of super-massive black holes. The remaining 80% is almost completely in gaseous form lying both within and between the galaxies and constitutes the reservoir from which future generations of stars may form. So the Universe will be able to form stars for approximately a further 70 billion years after which it will start to go dark.

The MGC was able to focus on the structures in which stars are arranged inside galaxies so their main components could be studied separately. The survey is the first to catalogue reliable information on the distances, sizes, colours and shapes of both the bulge and disc components of so many galaxies. On average it was found that half the stars in the Universe lie in the central bulges of galaxies, while the other half are found in discs surrounding the bulges. By measuring the concentration of stars in each galaxy's bulge, the super-massive black hole mass at the heart of each galaxy could also be determined.

FROM SPIRALS TO SMOOTH DISKS

Over the past several billion years the predominant shape of disc galaxies in clusters has changed from a spiral to a smooth disk. Theory suggests that this change occurs when two galaxies of unequal mass merge and gravitational effects pull gas to the galaxies' nucleus, sweeping away the spiral structure and leaving behind a smooth, barren, thickened disk known as a lenticular galaxy. However, galaxies orbiting in clusters move at high speeds and in random directions, which should mean that the conditions needed for these slow interactions rarely occur. Instead, multiple rapid encounters between galaxies, known as 'galaxy harassment', are dominant but these types of fast encounters cannot easily form the smooth disks.

Astronomers using imaging data from the JKT compared eight examples of populations of galaxies falling towards the centres of galaxy clusters with control samples of galaxies far from the clusters. They found that the infalling galaxies in the cluster were predominantly distorted in shape and had higher than normal rates of star formation. Between a half and three-quarters of these galaxies were very close by to another galaxy or appeared to be merging with a companion galaxy, which suggested that

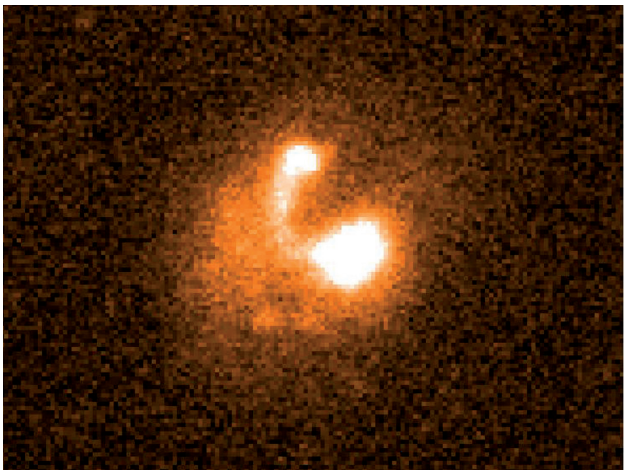

Figure 23. R-band image of CGCG 538-043 in Abell 347 (z=0.019) obtained with the JKT. This image resolves the galaxy into an interacting pair of galaxies. Credit: C. Moss, C.F. Thomas, P.A. James, Astrophysics Research Institute, Liverpool John Moores Univ.

interactions and mergers are more common in galaxies falling into the cluster than in the control sample. The results suggest that the conditions needed for slow galaxy interactions and mergers are more likely to occur in galaxies falling into a galaxy cluster compared to the general population of galaxies outside clusters.

And this may explain the mystery of how spiral galaxies in clusters are transformed over time into smooth disks: the slow-motion conditions needed for the transformation are indeed occurring among populations of galaxies falling towards the cluster centre.

Since infalling of galaxies into clusters was greater in the past, such interactions and mergers may have contributed significantly to the transformation of the past population of cluster spirals to lenticular galaxies in present-day clusters, explaining why clusters today have so few spirals and so many lenticular galaxies.

ANDROMEDA X: A NEW DWARF SPHEROIDAL SATELLITE OF M31

In hierarchical cold dark matter (CDM) models, large galaxies like the Milky Way and M31 form from the merger and accretion of smaller systems. Such models, while successful at large scales, predict at least 1–2 orders of magnitude more low-mass dark subhalos at the present epoch than the observed abundance of dwarf galaxies. This discrepancy, the "missing satellite" problem, is one of the most serious obstacles for matching CDM theory to observations.

A number of solutions have been proposed to address the problem, at least qualitatively. These range from the possibility that small galaxies somehow inhibit star formation, making them essentially invisible, to the prospect that they are surrounded by more unseen dark matter than first thought. All of these solutions aim to resolve the discrepancy between theory and observation by creating models that predict fewer directly observable satellites.

A complementary observational approach would be to place more stringent constraints on the faint end of the galaxy luminosity function, but attempts to do so are hampered by the low surface brightness expected of galaxies in that regime. The advent of wide-field CCD surveys such as the Sloan Digital Sky Survey (SDSS) has made it possible to detect stellar structures with extremely low surface brightness, and in 2004 astronomers discovered the two faintest galaxies ever seen – UMajor

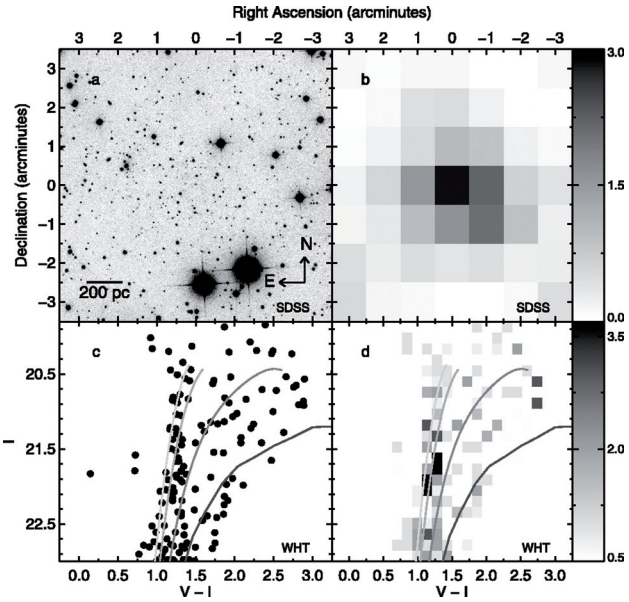

Figure 24. Andromeda X as seen by the SDSS and WHT: (a) Sum of SDSS g, r, and i images centered on And X. (b) Spatial density of presumed SDSS "blue" red giant stars in the same area, binned 1'×1' FWHM Gaussian. The gray-scale bar to the right indicates the significance of the spatial overdensity, in units of the background standard deviation. (c) De-reddened WHT CMD of stars within 2' of the center of And X with fiducial sequences overplotted for Galactic globular clusters with metallicities of (left to right) [Fe/H] = –2.2 (M15), –1.6 (M2), –0.7 (47 Tuc), and –0.3 (NGC 6553), shifted to a distance modulus of 24.47. (d) De-reddened WHT Hess diagram of stars within 2' of the center of And X, minus the area-scaled Hess diagram of a control field. The data are binned by 0.15 mag in (V-I) and I. The gray-scale bar indicates the number of stars in each bin. Overplotted fiducials are as for (c) (figure from Zucker et al., 2007, ApJL, 659, 21).

around our Milky Way and Andromeda IX (And IX) around our nearest large galactic neighbour, Andromeda. These finds suggested that the missing satellite problem may actually be less dire than originally thought.

Since the discovery of And IX, astronomers have been using SDSS photometry of M31 and its surroundings to identify possible M31 companions for deeper observations on other telescopes. Using data from PFIP on the WHT, a team of astronomers reported the discovery of a new dwarf spheroidal companion to M31, Andromeda X (And X), comparable in luminosity to And IX. They estimated its distance and other physical properties, and found that And X has a de-reddened central surface brightness of $\mu_{V,0}$~26.7 mag arcsec^{-2} and a total apparent magnitude of V_{tot} ~16.1, which at the derived distance modulus $(m-M)_0$~24.12–24.34, yields an absolute magnitude of M_V~–8.1±0.5. These values are similar to those of And IX.

And X is comparable in size, surface brightness, and apparent magnitude to And IX, and, despite the uncertainty

in its distance, And X appears to be somewhat lower in luminosity. So astronomers concluded that And X is a new extremely faint dSph companion of M31. The earlier discovery of And IX raised the question of whether such low-luminosity galaxies were a rarity in the Local Group or whether And IX was the tip of an iceberg, one of a large population of faint satellites that have thus far remained undetected. And X's discovery, along with the recent discoveries of numerous other faint dwarfs around the Milky Way and M31, suggests that the latter scenario is closer to the truth —that M31 and the Milky Way have a large number of low-luminosity satellites.

NON-CIRCULAR MOTION AND A GALACTIC WIND IN THE CENTRAL REGION OF M100

Departures from regular rotation, such as winds, elongated orbits or streaming motions, provide useful information about the dynamics and history of galaxies. To identify kinematical distortions and to infer how they relate to the gravitational potential, different techniques such as velocity field fitting or Fourier analysis can be used. However, to obtain reliable results these tools must be used in combination with 2D kinematical data of high spatial resolution. Integral-field spectroscopy (IFS) is an observational technique especially suited for kinematical studies that can be applied to nearby galaxies, such as M100 (NGC 4321), to obtain velocity maps with detailed spatial information.

The inner region of M100 has been extensively studied at different wavelengths, which has revealed some interesting irregular features. On the one hand, the inner region of this galaxy shows a peculiar morphology that is quite different in the optical and in the NIR. In the optical (broad-band), the structure is dominated by two spiral arms and an oval-shaped region of enhanced star formation, while the NIR shows an inner bar aligned with the large-scale stellar bar and a pair of small arms emerging from its ends. Whether there is a single bar or two nested bars that just happen to be aligned has been a greatly debated issue. On the other hand, non-circular motions observed from Hα data, have been interpreted as the kinematical signatures of gas streaming along the inner part of the bar, and of dense wave streaming motions across a two-armed mini spiral. Relevant pattern speeds of this galaxy have been measured at a larger scale by different methods. Recently, data obtained on the inner region of M100 using SAURON at the WHT confirmed that the star formation ring is formed by young stars, but they also revealed a low gas velocity dispersion compared to the surroundings.

Astronomers using INTEGRAL on the WHT observed the central 2.5 kpc of M100 and obtained data on the stellar and ionised gas velocity fields to analyse the symmetries of the departures from pure rotation and to estimate the nuclear bar pattern speed. Fourier analysis of the velocity residuals obtained by subtracting an axisymmetric rotation model from the Hα velocity field indicates that the distortions are global features, generated by an m=2 perturbation of the gravitational potential and can be explained by the nuclear bar. This bar has been previously observed in the near-infrared but not in the optical continuum dominated by star formation. The detection of the optical counterpart of this bar in the 2D distribution of the old stellar population and its analysis using the Tremaine–Weinberg method, allowed the determination of the pattern speed of the inner bar, obtaining a value of Ω_b= 160 ± 70 km s^{-1} kpc^{-1} . This value is considerably larger than the one obtained when a simple bar model is considered.

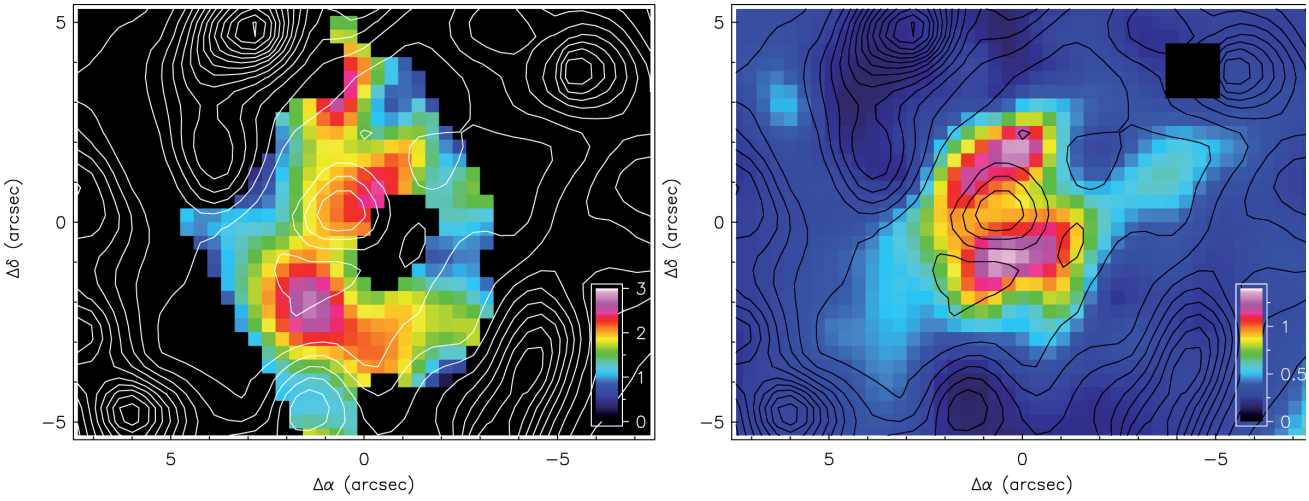

Figure 25. [NII]/Hα line ration for the wind (left) and Galactic (right) components. Contours show intensity of galactic Hα emission (figures from Jiménez-Vicente et al., 2007, MNRAS, 382, L16).

Galactic winds are one of the main mechanisms by which galaxies expel metals, dust, cosmic rays, magnetic fields, etc, to the intergalactic medium. This feedback makes winds an important phenomenon in our global understanding of galaxies. These winds are usually associated with galaxies with strong nuclear activity or with starbursts, which are powerful enough to feed the winds. However, very little is known of this phenomenon in quiescent, inactive galaxies. M100 is a nearby galaxy with low nuclear activity and a moderate star formation rate of a few solar masses per year. Despite this apparent quiescence, astronomers using INTEGRAL on the WHT found an unexpected fast wind emanating from its nuclear region.

They used a new approach based on integral field spectroscopy which allows both the detection of absorbing material throughout the field of view and the production of a map of the distribution and kinematics of the absorbers. In addition, they could discriminate kinematically the ionised component of the outflowing material and to produce maps for the distribution and kinematics of this hotter phase of the wind. This approach provides a unique simultaneous global view of these two phases of a galactic wind.

The primary evidence of the wind is the presence of blueshifted interstellar NaD absorption lines. The velocity field of the absorbers show a clear rotation pattern but which is globally blueshifted (~ –115 km s^{-1}) with respect to the systemic velocity of the galaxy. The emission lines also present a blueward component arising from the ionised gas phase of the galactic wind. The velocity field of the ionised gas wind component shows no evidence of rotation but exhibits a pattern that can be interpreted in terms of the projection of an outflowing cone or shell. The wind component has [N II]/Hα ratios of about 1.8, typical of shock ionisation.

The ionised component of the wind can be identified with an expanding shell of shocked gas, and the neutral component with disc gas entrained in the wind at the interface of the expanding shell with the galactic interstellar medium. The galactic wind seems to be driven uniquely by the nuclear starburst. The analysis indicates that a non-negligible fraction of the wind material might escape to the intergalactic medium (IGM). In this case, if the wind detected in M100 were representative of similar phenomena in other galaxies with low to moderate activity, the current estimates of metal and dust content of the IGM might be drastically underestimated.

THE METALLICITY GRADIENTS OF M 33

The galaxy M33 (NGC 598) is the third-brightest member of the Local Group. Its proximity, its large angular size, and its intermediate inclination make it particularly suitable for studies of spiral structure, interstellar medium (ISM), and of stellar populations. Being a late-type spiral galaxy, it has a rich population of H II regions. Observations with the INT, covering an area of approximately 0.6 square degrees, produced the most complete catalogue of H II regions in this galaxy.

ING's Local Group Census project (LGC) obtained new imaging observations of M33. These new deep data cover about 2 square degrees and are allowing discovery of a conspicuous number of new H II regions at large galactocentric distances. The existence of chemical abundance gradients in M33 was known long ago, but their origin, shape and magnitude are still open issues.

Using AF2 on the WHT, a team of astronomers investigated the chemical and physical properties of a large sample of H II regions of different sizes, galactocentric distances and excitations in order to study their behaviour through the disk.

In total, they analysed optical spectra of 72 emission-line objects in M33, including mostly H II regions, but also five supernova remnants and two candidate planetary nebulae. Direct determination of electron temperature was possible for 15 H II regions by the measurements of the [O III] 436.3 nm line and in three of them using the [N II] 575.5nm line. For the 14 H II regions with a determined electron temperature and with detection of both [O II] and [O III] lines they derived chemical abundances.

They also collected oxygen abundances from young stars presented in a large number of objects representative of the present time interstellar medium metallicity to draw a complete picture of the shape and magnitude of the metallicity gradient, and they found the best fit to the data using two different slopes, corresponding to the central regions R<3 kpc (–0.19±0.08 dex kpc^{-1}) and outer regions R=3kpc (–0.038 ±0.015dex kpc^{-1}). The shallower outer gradient is in agreement with several new works and it can be explained by invoking a slow continuous accretion of the disk of M33 from the intergalactic medium that continues to the present time.

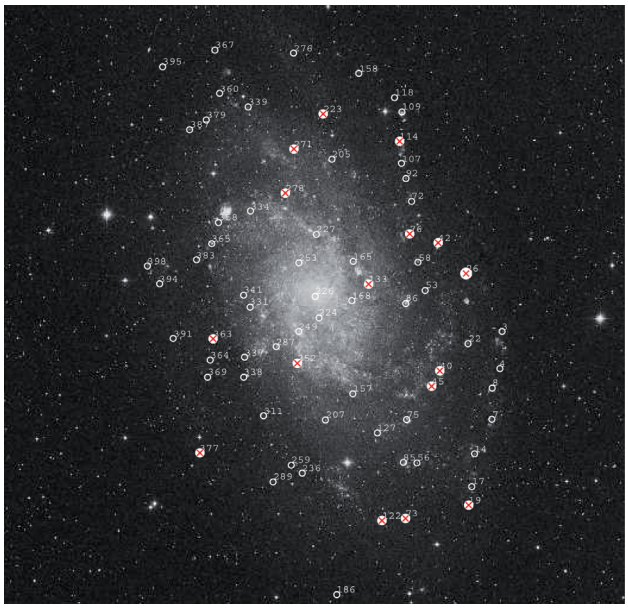

Figure 26. M33 DSS 1°×1° image indicating the location of the 72 observed emission-line objects (North is up and East to the left). HII regions with measured chemical abundances are marked with a cross (figure from Magrini et al., 2007, A&A, 470, 865).

THE SAURON PROJECT

SAURON (Spectroscopic Areal Unit for Research on Optical Nebulae) is a panoramic integral-field spectrograph built for the WHT by groups in Leiden, Lyon and Oxford. SAURON can record 1577 spectra simultaneously, with full sky coverage in a field of 33×44 arcmin and it was used to measure the kinematics and line strength distribution for a representative sample of 72 nearby early-type galaxies (ellipticals, lenticulars, and Sa bulges, in clusters and in the field).

In parallel with the data taking, the team developed a number of tools that are the key to analysing all the resulting maps, and in particular they built an elaborate software pipeline to reduce and analyse the data which produces full 2D maps of velocity from both stellar absorption lines and ionised gas emission lines, of velocity dispersion and of line ratios.

SAURON saw first light at the WHT in 1999. The entire survey was completed in 2003, and the instrument continued operations in the following years. Up to 2007, the SAURON collaboration had published more than 10 research papers covering different aspects of the research. What follows is a summary of the papers published in 2006 and 2007.

A study dealing with the fundamental plane of early-type galaxies showed that the scatter in the mass-to-light ratio vs. galaxy mass relation was extremely small, and that small ellipticals in their central regions have almost no dark matter.

A second paper showed that early-type galaxies contain large amounts of ionised gas, in many cases in regular, stable orbits, but in other cases showing signs of infall.

A third paper provided 2D absorption line strength indices for the elliptical and S0 galaxies in the survey. Another work provides velocity and velocity dispersion fields for gas and stars in the 24 early-type spirals of the SAURON survey. A major result is that many of these objects have central disks dominating the light there. The kinematics of gas and stars and absorption line strength maps for a large fraction of these galaxies, and a number of newly discovered kinematically decoupled cores, were presented in another paper.

Two-dimensional stellar kinematics of 48 representative elliptical and lenticular galaxies revealed that early-type galaxies appear in two broad flavours, depending on whether they exhibit clear large-scale rotation or not.

A kinematical analysis of the orbital distribution of elliptical and lenticular galaxies kinematics within about one effective (half-light) radius showed that of two classes, the slow rotators are more common among the most massive systems and are generally classified as ellipticals from photometry alone. Those in the analysed sample tend to be fairly round, but can have significant kinematical misalignments, indicating that as a class they are moderately triaxial; the fast rotators are generally fainter and are classified as either elliptical or lenticular. They can appear quite flattened and do not show significant kinematical misalignments (unless barred or interacting), indicating that they are nearly axisymmetric and span an even larger range of anisotropies.

A number of the fast rotators show evidence for containing a flattened, kinematically distinct component, which in some cases counter-rotates relative to the main galaxy body. These components are generally more metal rich than the galaxy body. All these results support the idea that fast rotators are nearly oblate and contain disc-like components. The role of gas must have been important for their formation. The slow rotators are weakly triaxial. Current collisionless merger models seem unable to explain their detailed observational properties.

The absorption-line strength maps of a sample of 24 representative early-type spiral galaxies, mostly of type Sa, showed that the central regions of Sa galaxies contain at least two components: a thin, disc-like component, often

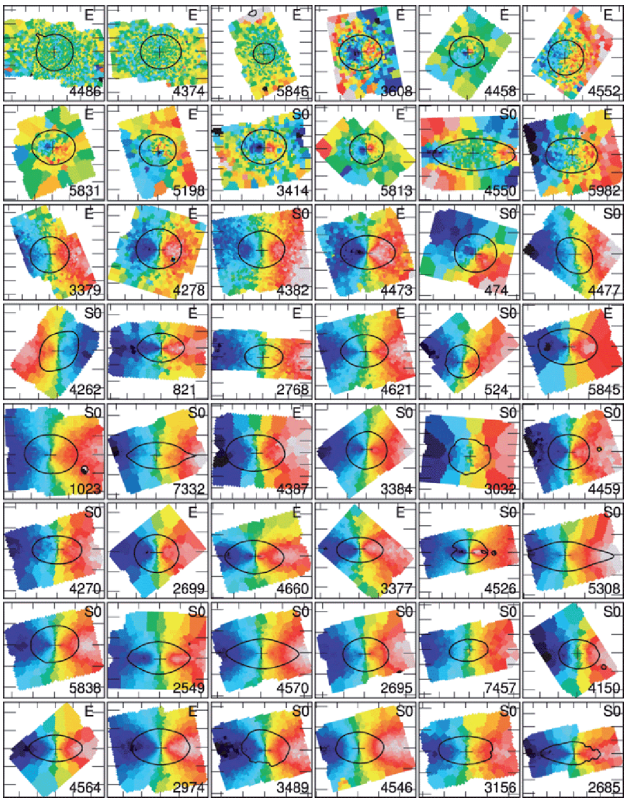

Figure 27. Example of SAURON project analysis: stellar velocity fields for 48 elliptical (E) and lenticulars (S0) galaxies, the global outer photometric axis being horizontal. Colour cuts were tuned for each individual galaxy as to properly emphasise the observed velocity structures. A representative isophote is overplotted on each thumbnail as a black solid line, and the centre is marked with a cross. Slow rotators are galaxies on the first two rows. NGC numbers and Hubble types are provided in the lower-right and upper-right corners of each panel, respectively. Tick marks correspond to 10 arcsec (figure from Emsellem et al., 2007, MNRAS, 379, 401).

containing recent star formation, and another, elliptical-like component, consisting of old stars and rotating more slowly, dominating the light above the plane. These components together form the photometrically defined bulge, in the same way as the thin and the thick disc co-exist in the solar neighbourhood. In this picture, part of the bulge, the thicker component, formed a very long time ago. Later, stars continued to form in the central regions of the disc, rejuvenating in this way the bulge through dynamical processes. This picture is able to explain, in a natural way, the heterogeneous stellar populations and star formation characteristics that we are seeing in detailed observations of early-type spiral galaxies.

THE PLANETARY NEBULA SPECTROGRAPH PROJECT

The confirmation in the 1970s that dark matter dominates the mass of the universe came from dynamical studies of spiral galaxies. In these systems, The H I gas disks offer the ideal diagnostic, since their extended nature allows one to probe very large radii where dark matter begins to dominate, and their cold disk-like structure ensures that the material is following approximately circular orbits, removing a major ambiguity in the study of its dynamics.

A similar study of elliptical galaxies would be invaluable, as it would address basic questions such as whether the dark matter halos around these systems are similar to those around spirals, suggesting that the difference in observed morphology is just a matter of chance, or that there are more fundamental differences between them. Unfortunately, the paucity of neutral hydrogen gas in ellipticals makes such a study observationally difficult.

The main object of the Planetary Nebula Spectrograph (PN.S) project is to determine whether or not the dark matter halos which are inferred to be present around spiral galaxies are also present in ellipticals. Earlier investigations, often based on the kinematics of a few tens of planetary nebulae, suggested that ellipticals contained significantly less mass than expected by the Cold Dark Matter (CDM) model of dark matter halos. The PN.S is specialised in the collection of the required planetary nebulae data and in 2003 a paper published in *Science* showed a preliminary analysis of three galaxies which supported the earlier findings.

In the consecutive years the project team continued to collect the data on a sample of 12 ellipticals, and by the start of 2006 had almost completed this process, and had begun analysing the data using an improved pipeline.

The first analysis to be published, which included all the technical data needed to scrutinise the data-reduction process for errors or biases, was that of the galaxy NGC3379, in which they obtained radial velocities for 214 planetary nebulae. The main conclusion of this work was that, barring the presence of a significant disk population hidden by a special viewing angle, disturbing the modelling of the planetary nebulae kinematics, the dark matter component within 5 effective radii cannot be greater than 40% of the total mass, whereas the CDM model predicts twice this.

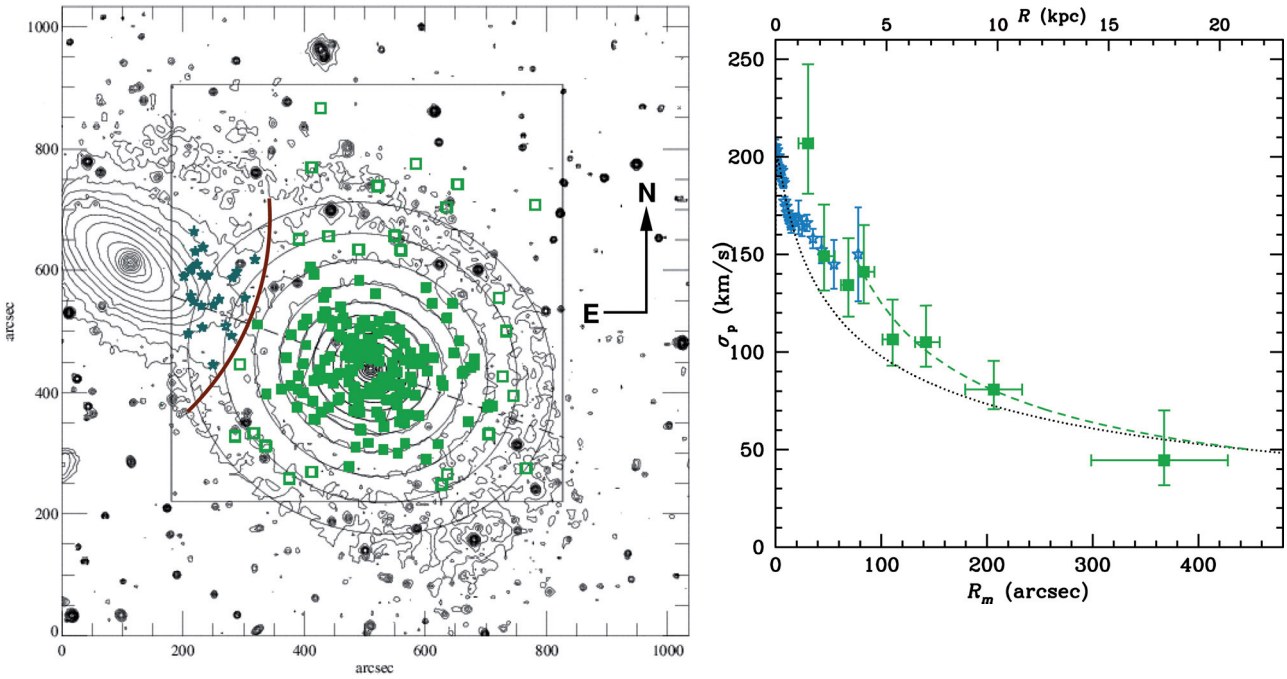

Figure 28. Left: I-band image with the locations of detected PNe and the field of the PN.S observation marked. The thick arc marks the division between the two galaxies for assigning membership to PNe, so squares are members of NGC 3379 while stars are members of NGC 3384. The filled symbols for NGC 3379 are used for objects that lie within the isophotal radius out to which the entire galaxy has been mapped. Right: Projected velocity dispersion profile for NGC 3379, showing data from stars (stars) and PNe (squares), plotted on linear axes. Dashed lines show a power-law fit at large radii, while dotted lines show an isotropic constant mass-to-light ratio model (figures from Douglas et al., 2007, ApJ, 664, 257).

DISCOVERY OF ULTRACOMPACT DWARF GALAXIES IN THE VIRGO CLUSTER

Compact dwarf galaxies are an established constituent of the population of lower luminosity galaxies, alongside the more numerous dwarf irregular, dwarf elliptical, and dwarf spheroidal galaxies. Among compact dwarfs, early-type compact elliptical galaxies such as M32, showing early-type galaxy spectra, are rare, and only very few examples have been found. Blue compact dwarfs show active star formation superposed on an older, low surface brightness component and have a broad range of sizes, including a very small proportion with effective radii as small as 300 pc.

Using follow-up data from the Wide Field Camera on the INT, astronomers discovered nine ultracompact dwarf galaxies (UCDs) in the Virgo Cluster, extending samples of these objects outside the Fornax Cluster. The newly found UCDs are comparable to the UCDs in the Fornax Cluster, with sizes ~<100 pc, -12.9<M_B < -10.7, and exhibiting red absorption-line spectra, indicative of an older stellar population. The properties of these objects remain consistent with the tidal threshing model for the origin of UCDs from the surviving nuclei of nucleated dwarf elliptical galaxies disrupted in the cluster core, but can also be explained as objects that were formed by mergers of star clusters created in galaxy interactions.

The discovery that UCDs exist in Virgo shows that this galaxy type is probably a ubiquitous phenomenon in clusters of galaxies; coupled with their possible origin by tidal threshing, the UCD population is a potential indicator and proof of the formation history of a given cluster.

KINEMATICS OF THE ANDROMEDA GALAXY

Observations of the distribution of stellar velocities in the solar neighbourhood of the Milky Way reveal a wealth of complex structure. For a dynamical entity such as the Galaxy, this structure is as fundamental as the spatial arrangement of its stars, and should contain a wealth of information as to the system's current state, as well as archaeological clues as to how it formed. Unfortunately, such data from a single locality are difficult to interpret in terms of the global structure of the Galaxy. Although kinematic observations of more distant stars in the Milky Way have been made, the complexity of disentangling the geometry of our own Galaxy makes such data difficult to interpret. An obvious next target is therefore the Milky Way's nearby sister system, the Andromeda galaxy, M31.

However, studying the detailed kinematics of stars in even a nearby external galaxy is quite challenging. In fact, the first problem arises from its very nearness: M31 subtends such a large angle on the sky that many spectroscopic

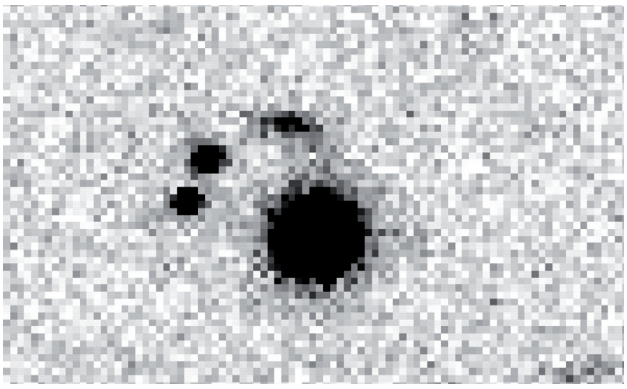

Figure 29. Region around Virgo UCD 6 is shown based on a 25 minute B-band integration with the INT Wide Field Camera (figure from Jones et al., 2006, AJ, 131, 312).

instruments are unable to survey the whole system within a realistic time. Further, even at what by extragalactic standards is a very modest distance, obtaining high-quality spectra of individual stars is challenging; it is only relatively recently that the requisite observations of even bright red giant branch (RGB) stars have been made.

Planetary nebulae (PNe) have long been recognised as a potentially simpler dynamic tracer of the stellar population. Stars evolve very rapidly but quite gently from the RGB phase to become PNe, so the kinematics of these two populations should be essentially identical. Further, the presence of strong emission lines in PNe make them quite easy to identify, and render the measurement of their Doppler shifts fairly trivial.

More than 20 years ago, astronomers reported on kinematic measurements of 34 PNe in M31, but it was not until recently with the development of wide-field multi-object spectrographs that it has become possible to start to obtain the large samples necessary for dynamical studies. Even with such instruments, these studies involve both narrow-band imaging to identify candidate PNe and subsequent spectral follow-up, and this complex two-stage process has limited astronomers' enthusiasm for such projects. However, the recently commissioned Planetary Nebula Spectrograph (PN.S) on the WHT has reduced this process to a single stage, simultaneously identifying PNe and measuring their velocities.

Astronomers have therefore used this instrument to carry out a deep kinematic survey of PNe over ~6 deg^2, covering the bulk of M31's visible area. They obtained a catalogue of positions, magnitudes and velocities for 3300 emission-line objects found by the PN.S. Of these objects, 2615 are found likely to be planetary nebulae (PNe) associated with M31. With the exception of the very central, high surface brightness region of M31, this survey is complete to a magnitude limit of m_{5007}~23.75, 3.5 mag into the PN luminosity function.

The calibrated data were checked for internal consistency and compared with other catalogues, in particular one made from observations previously obtained using AF2 on the WHT and narrow-band imaging with the Wide Field Camera on the WHT. This comparison survey had produced a sample of 723 PNe in the disc and bulge of M31. Velocities were determined using the [O III] λ5007 emission line. Rotation and velocity dispersion were measured to a radius of 50 arcmin (11.5 kpc), resulting in the first stellar rotation curve and velocity dispersion profile for M31 out to such a radius. The kinematics were consistent with rotational support at radii well beyond the bulge effective radius of 1.4 kpc, although the data beyond a radius of 5 kpc were limited.

The luminosity function of the surveyed PNe is well matched to the usual smooth monotonic function. The only significant spatial variation in the luminosity function occurs in the vicinity of M31's molecular ring, where the luminosities of PNe on the near side of the galaxy are systematically ~0.2 mag fainter than those on the far side. This difference can be explained naturally by a modest amount of obscuration by the ring. The absence of any difference in luminosity function between bulge and disc suggests that the sample of PNe is not strongly populated by objects whose progenitors are more massive stars. This conclusion is reinforced by the excellent agreement between the number counts of PNe and the *R*-band light.

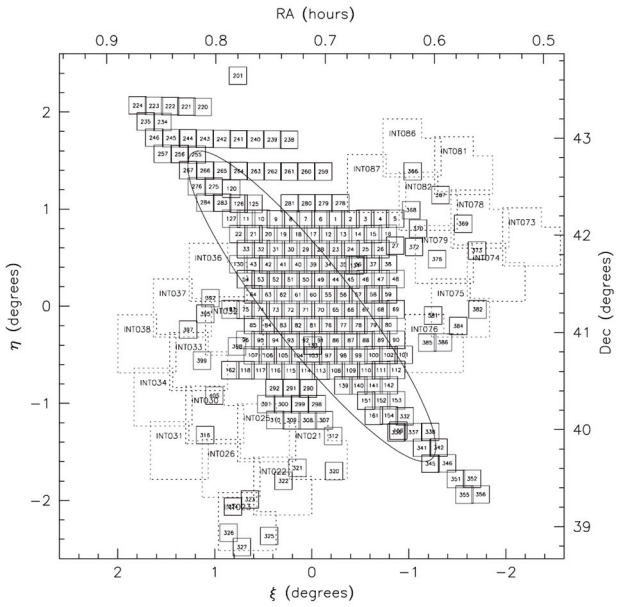

Figure 30. Fields observed in M31. The small square fields are PN.S field locations; the larger fields with dotted outlines are the INT WFC fields. The ellipse marks a 2° (27.4 kpc) disc radius (figure from Merrett et al., 2006, MNRAS, 369, 120).

The number counts of kinematically selected PNe also allows to probe the stellar distribution in M31 down to very faint limits. There is no indication of a cut-off in M31's disk, out to beyond four scale lengths, and no signs of a spheroidal halo population in excess of the bulge out to 10 effective bulge radii.

A preliminary analysis of the kinematics of the surveyed PNe shows that the mean streaming velocity of the M31 disc PNe reveals a significant asymmetric drift out to large radii. Their velocity dispersion, although initially declining with radius, flattens out to a constant value in the outer parts of the galaxy. There are no indications that the disc velocity dispersion varies with PN luminosity, once again implying that the progenitors of PNe of all magnitudes form a relatively homogeneous old population. The dispersion profile and asymmetric drift results are shown to be mutually consistent, but require that the disc flares with radius if the shape of its velocity ellipsoid is to remain invariant.

THE POINT-AGAPE SURVEY

The POINT-AGAPE (Pixel-lensing Observations with the Isaac Newton Telescope-Andromeda Galaxy Amplified Pixels Experiment) survey is an optical search for gravitational microlensing events towards the Andromeda galaxy (M31). As well as microlensing, the survey is sensitive to many different classes of variable stars and transients.

The POINT-AGAPE collaboration monitored M31 for three seasons (1999-2001) with the Wide Field Camera on the INT. In each season, data were taken for one hour per night for roughly 60 nights during the six months that M31 was visible. The two 33×33 arcmin^2 fields of view straddle the central bulge, northwards and southwards.

The galactic dark matter may be partly composed of compact objects (e.g., black holes, faint stars, brown dwarfs, jupiters) that reside in halos and are popularly called MACHOs ("MAssive Compact Halo Objects"). Observations toward the Magellanic Clouds by the first generation of microlensing surveys yielded important constraints on the Milky Way (MW) halo. The EROS collaboration obtained an upper limit to the contribution by MACHOs to a standard MW halo. Also, according to the MACHO collaboration, the optical depth toward the Large Magellanic Cloud is too large by a factor ~5 to be accounted for by known populations of stars. This excess is attributed to MACHOs of mass ~0.4 solar masses (in the mid-range of mass for main sequence stars).

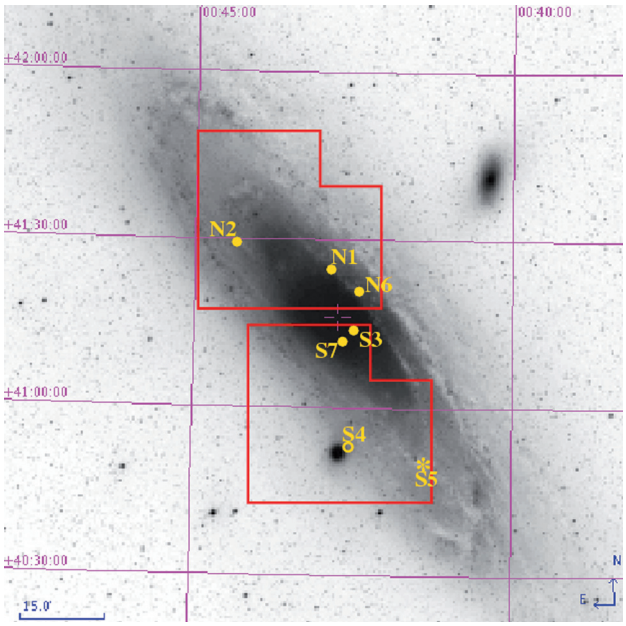

Figure 31. The boundaries of the observed fields are marked as red lines, and the centre of M 31 is a cross. Circles mark the positions of the 6 microlensing events detected. The open circle (S4) corresponds to an event seen toward M32. The star (S5) indicates the position of a binary event candidate (figure from Calchi Novati et al., 2005, A&A, 443, 911).

M 31, being both nearby and similar to the MW, is a suitable target for such a search. It allows observers to explore the MW halo along a different line of sight. It has its own halo that can be studied globally, and its high inclination is expected to give a strong gradient in the spatial distribution of microlensing events. However, the latter feature, which was at first believed to provide an unmistakable signature for M 31 microlensing halo events, seems to be shared, at least to some extent, by the variable star population within M 31.

A high-threshold analysis of the 3 years of data yielded 6 bright, short-duration microlensing events, which are compared with a simulation of the observations and the analysis. The observed signal is much larger than expected from self lensing alone and the astronomers conclude, at the 95% confidence level, that at least 20% of the halo mass in the direction of M 31 must be in the form of MACHOs if their average mass lies in the range 0.5-1 solar masses. This lower bound drops to 8% for MACHOs with masses ~0.01 solar masses.

In addition, they found a likely binary microlensing candidate with a caustic crossing. Its location, some 32 arcmin away from the centre of M31, supports the conclusion that they were detecting a MACHO signal in the direction of M31.

The POINT-AGAPE survey also yielded the identification of 20 classical novae (CNe) candidates observed over three seasons in M31. CNe were detected both in the bulge region as well as over a wide area of the M31 disc. Nine of the CNe were caught during the final rise phase and all are well sampled in at least two colours. The excellent light-curve coverage allowed the astronomers to detect and classify CNe over a wide range of speed class, from very fast to very slow. Among the light curves is a moderately fast CN exhibiting entry into a deep transition minimum, followed by its final decline. The CN catalogue constitutes a uniquely well-sampled and objectively-selected data set with which to study the statistical properties of CNe in M31, such as the global nova rate, the reliability of novae as standard-candle distance indicators and the dependence of the nova population on stellar environment.

A catalogue with the locations, periods and brightness of 35,414 variable stars in M31 was produced as a by-product of the microlensing search. The variables were classified according to their period and brightness. Rough correspondences with classical types of variable star (such as Population I and II Cepheids, Miras and semi regular long-period variables) were established. The spatial distribution of Population I Cepheids is clearly associated with the spiral arms, while the central concentration of the Miras and long-period variables varies noticeably, the brighter and the shorter period Miras being much more centrally concentrated.

A crucial role in the microlensing experiment is played by the asymmetric signal – the excess of events expected in the southern or more distant fields as measured against those in the northern or nearer fields. It was initially assumed that the variable star populations in M31 would be symmetric with respect to the major axis, and thus variable stars would not be a serious contaminant for measuring the microlensing asymmetry signal. However, it was found that all the variable star distributions are primarily asymmetric because of the effects of differential extinction associated with the dust lanes.

A PANORAMA OF ANDROMEDA AND TRIANGULUM HALOS

The outskirts of galaxies hold fundamental clues about their formation history. It is into these regions that new material continues to arrive as part of their ongoing assembly, and it was also into these regions that material was deposited during the violent interactions in the galaxy's distant past. Moreover, the long dynamic timescales for structures beyond the disk ensure that the debris of accreted material takes a very long time to be erased by the process of phase mixing, which in turn means that it is possible to detect many of these signatures of formation as coherent spatial structures.

Much theoretical effort has been devoted in recent years to understanding the fine-scale structure of galaxies, as researchers realised that cosmological models could not only be tested with the classical large-scale probes, such as galaxy clusters, filaments, and voids, but also with observations on galactic and subgalactic scales. Indeed, it is precisely in the latter regions that the best constraints on cosmology are expected to be placed in the coming decades. The ΛCDM cosmologies, in particular, are now sufficiently well developed theoretically that the Local Group provides a means of directly testing and constraining these theories, by observing the profiles of density, age, and metallicity of the structure and substructure predicted to be found in the outer parts of galaxy disks and in galaxy halos.

Andromeda, like the Milky Way, is a canonical galaxy and a laboratory for examining in close detail many of the astrophysical processes that are investigated in the more distant field. Studying Andromeda and Triangulum in the Local Group has the advantage that it affords us a view free from the problems that plague Galactic studies due to our position within the Milky Way, yet their location within the Local Group allows us to resolve and study individual stars and deduce population properties in incomparably greater detail than is possible in distant systems.

Andromeda is the closest giant spiral galaxy to our own and the only other giant galaxy in the Local Group. In many ways Andromeda is the “sister” to the Milky Way, having a very similar total mass, having shared a common origin, and probably sharing the same ultimate fate when they finally merge in the distant future. However, there are significant differences between these “twins.” M31 is slightly more luminous than the Milky Way, and it has a higher rotation speed and a bulge with a higher velocity dispersion. M31 possesses a globular cluster system with ~500 members, approximately 3 times more numerous than that of the Milky Way.

The disk of Andromeda is also much more extensive, but is currently forming stars at a lower rate than the Galaxy. There are indications that the Milky Way has undergone an exceptionally low amount of merging and has unusually low specific angular momentum, whereas M31 appears to be a much more normal galaxy in these respects. Although possibly the consequence of low number statistics, it is

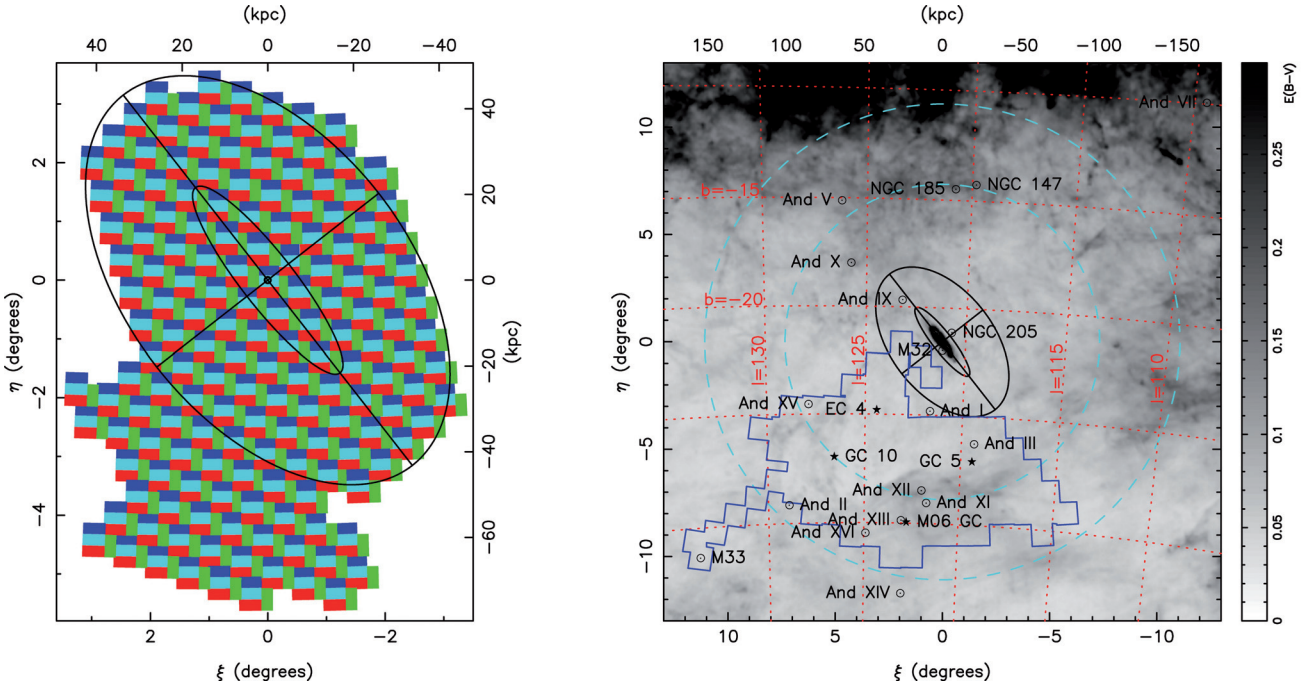

Figure 32. Left: coverage of the large panoramic survey of M31 with the INT Wide Field Camera, in standard coordinates (ξ, η). The inner ellipse represents a disk of inclination 77° and radius 2° (27 kpc), the approximate end of the regular H I disk. The outer ellipse shows a 55 kpc radius ellipse and the major and minor axes are indicated with straight lines out to this ellipse. This map is constructed from a total of 164 INT WFC individual pointings. Right: survey region (irregular blue polygon) overlaid on a schematic diagram of M31 and surrounding Local Group structure. Note that the survey extension along the M31 minor axis reaches M33 and therefore probes the halos of both these disk galaxies. In addition to the ellipses reproduced on the left-hand figure, the two concentric dashed circles show projected radii of 100 and 150 kpc. A grid in Galactic longitude and latitude has been marked. The extinction over the surveyed region is also shown (figures extracted from Ibata et al., 2007, ApJ, 671, 1591).

tempting to attribute significance to the fact that Andromeda has a compact elliptical (M32) and three dwarf elliptical galaxies (NGC 205, NGC 147, NGC 185) among its entourage of satellites, as well as no star-forming dwarf irregulars (dIrrs) within 200 kpc, whereas the Milky Way has no ellipticals but two dIrrs. However, it is perhaps in their purported halo populations that the differences between the two galaxies are most curious and most interesting.

If Andromeda is the twin of the Milky Way, the Triangulum galaxy (M33), with a mass ~10 times lower than either of these two giants, is their little sister. M33 is the third brightest galaxy in the Local Group and probably a satellite of M31. The relatively undisturbed optical appearance of M33 places strong constraints on the past interaction of these two galaxies, although it should be noted that the gaseous component is extremely warped.

In order to study in more detail the halos of both the Andromeda and Triangulum galaxies, astronomers performed a deep photometric survey of the Andromeda galaxy, conducted with the Wide Field Camera of the INT and MegaCam on CFHT, that covered the inner 50 kpc of the galaxy and the southern quadrant out to ~150 kpc and included an extension to M33 at >200 kpc. This is the first

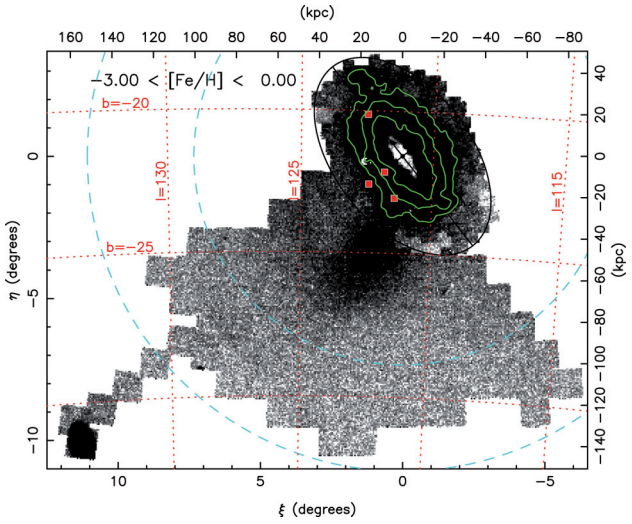

Figure 33. Matched filter map to the limiting depth of the INT survey (i_0=22.8 for S/N~10). The contours show the approximate location of the surface brightness levels 27, 28 and 29 mag arcsec^{-2} respectively (figure from Ibata et al., 2007, ApJ, 671, 1591).

systematic panoramic study of this very outermost region of galaxies. They detected a multitude of large-scale structures of low surface brightness, including several streams, and two new relatively luminous dwarf galaxies: And XV and And XVI.

Significant variations in stellar populations due to intervening stream–like structures are detected in the inner halo. Underlying the many substructures lies a faint, smooth, and extremely extended halo component, reaching out to 150 kpc, whose stellar populations are predominantly metal-poor. They find that the smooth halo component in M31 has a radially decreasing profile that can be fitted with a Hernquist model of immense scale radius ~55 kpc, almost 4 times larger than theoretical predictions. If it is symmetric, then the total luminosity of this structure is ~10^9 solar luminosities, again similar to the stellar halo of the Milky Way.

This vast, smooth, underlying halo is reminiscent of a classical "monolithic" model and completely unexpected from modern galaxy formation models. M33 is also found to have an extended metal-poor halo component, which can be fitted with a Hernquist model, also of scale radius ~55 kpc. These extended slowly decreasing halos provide a challenge and strong constraints for further modelling.

ECLIPSING BINARIES AND CEPHEIDS IN THE ANDROMEDA GALAXY

Cepheids are probably the most studied variable stars. Their large amplitudes and intrinsic luminosities make them easily detectable in most photometric variability surveys. In addition, their well-known period-luminosity (P-L) relationship has made these variable stars one of the main cornerstones in deriving extragalactic distances. The importance of Cepheids for distance determination stands in contrast with the relative lack of additional information on the specific characteristics of extragalactic Cepheids and the possible corrections because of their particular properties (i.e., metallicity).

A clear example is the Andromeda galaxy (M 31), where the first identification of Cepheids was already performed by Hubble in 1929. After the observations of Baade & Swope in 1965, few efforts have been dedicated to further analyse the Cepheid population in M 31.

This trend has changed in recent years with the emergence of new observational capabilities. Several variability surveys have started to study the stellar content in M 31 and other Local Group galaxies, obtaining large samples of Cepheids with accurate photometry. The detailed study of the observed Cepheids has emphasised the importance of an issue that was usually overlooked in most photometric studies, the effect of blending. It has been proposed that the magnitude of Cepheids may be affected by the light of unresolved companion stars (i.e., blends). The effect of blending is somewhat different from crowding or confusion noise, since companion stars appear to be in the same point-like source. Therefore, even when achieving perfect point-spread function modelling, blending can still be present. The effect can be the same as in spectroscopic binaries, where the individual components cannot usually be resolved from ground-based images.

With the goal of obtaining accurate distance determinations to the Andromeda Galaxy, and constraining the age and evolution of the Universe, astronomers started a project to use eclipsing binaries as distance indicators to M 31. Eclipsing binaries have been proved to yield direct and precise distances that are essentially assumption-free. To do so, high-quality photometric and spectroscopic data were needed. As a first step in the project, broad band photometry (in Johnson *B* and *V*) was obtained in a region (~34'×34') in the north eastern quadrant of the galaxy over 5 years.

The data, containing more than 250 observations per filter, generated a catalogue with 236,238 objects with photometry in both B and V passbands. This catalogue is the deepest (V<25.5 mag) photometric survey obtained so far in the studied region and it contains 3964 identified variable stars, with 437 eclipsing binaries and 416 Cepheids.

The most suitable eclipsing binary candidates for distance determination were selected according to their brightness and from the modelling of the obtained light curves. The resulting sample includes 24 targets with photometric errors around 0.01 mag. Detailed analysis (including spectroscopy) of some 5-10 of these eclipsing systems should result in a distance determination to M 31 with a relative uncertainty of 2-3% and essentially free of systematic errors, thus representing the most accurate and reliable determination to date.

The resulting sample of 416 Cepheids is the most complete in M 31 and has almost the same period distribution as the David Dunlap Observatory sample in the Milky Way. The large number of epochs (~250 per filter) has permitted the characterisation of the pulsation modes of 356 Cepheids, with 281 of them pulsating in the fundamental mode and 75 in the first overtone.

The findings show that the blending contribution is as important as the metallicity correction when computing Cepheid distance determinations to M 31 (~0.1 mag). Since large amplitude Cepheids are less affected by blending,

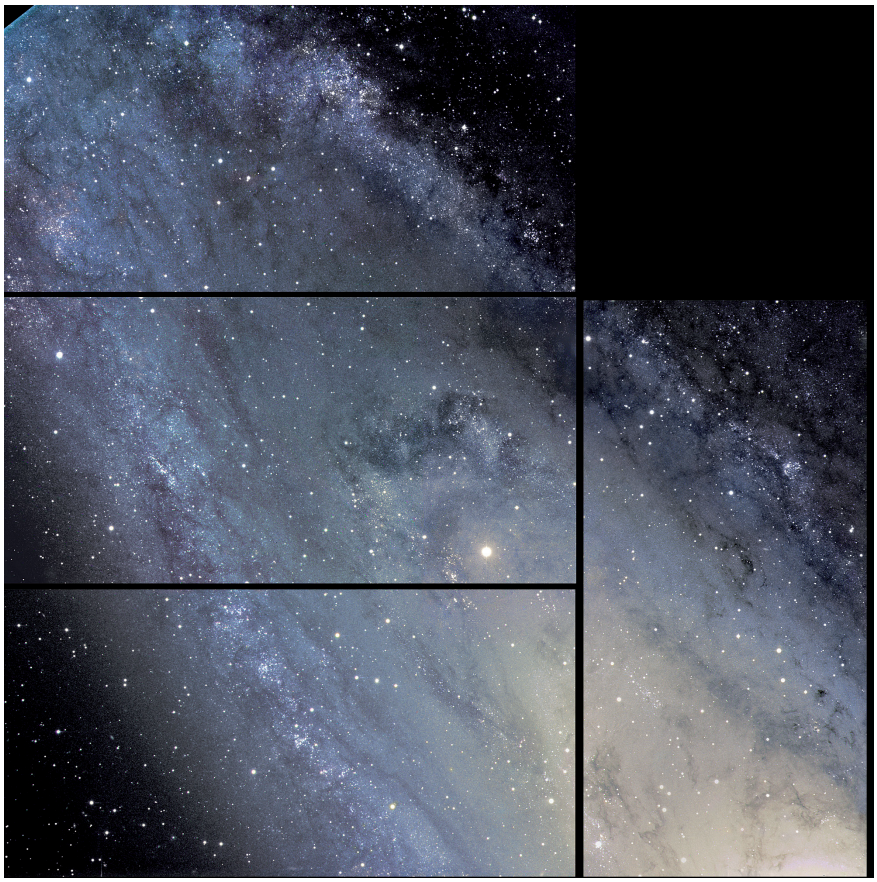

Figure 34. This INT Wide Field Camera composite image in B and V bands of the Andromeda Galaxy centered at R.A.=00h44m46s and Dec.=+41°38'20" shows the field of view used in the present study. (Credit: F. Vilardell, I. Ribas and C. Jordi, final image preparation by N. Szymanek)

they used those with an amplitude larger than 0.8 mag to derive a distance to M 31 of $(m\text{-}M)_0$=24.32±0.12 mag.

PROBING COSMIC EVOLUTION WITH GAMMA-RAY BURSTS

Gamma-ray bursts (GRBs) are very bright flashes of radiation, which are detected approximately 100 times per year by satellites. For a long time it was a mystery as to where these flashes originated from and how they were produced. In 1997 astronomers using the WHT discovered that GRBs show a so-called "afterglow": radiation in other wavelengths following the gamma-rays. This afterglow can be studied with telescopes from the Earth, and allowed astronomers to find that GRBs originate in the violent deaths of massive stars, in star-forming galaxies far away.

GRBs have proven to be excellent probes of the distant Universe. The high luminosities of GRB afterglows allow absorption line studies of the interstellar medium at high redshift up to redshifts larger than 6. The decrease in brightness of GRB afterglows means that a rapid response is essential, the afterglow can be "caught" when it is still bright. To exploit this benefit, the override programmes on the WHT and the INT are ideal for responding rapidly.

Early in the morning of February the 6th, 2006 a GRB was detected by the Swift satellite. The GRB was at that time high in the sky over La Palma and the weather was good. Within 15 minutes the NOT was pointed towards this burst by the Danish GRB follow-up group. Using ALFOSC a bright optical afterglow was discovered in the *R* band. Directly after the detection had been made, a low-resolution spectrum was acquired using the same instrument. The latter spectrum rapidly determined the redshift of GRB 060206 at z=4.048. Meanwhile, the WHT had been alerted through a collaboration of the NOT and WHT, involving GRB follow-up teams from the Netherlands, the United Kingdom and Denmark. Starting at just 1.6 hours after the burst a medium-resolution spectrum could be obtained using the WHT's ISIS spectrograph.

The combination of the NOT and WHT data provided a unique window on this afterglow. The low resolution and broad wavelength coverage of the NOT spectrum allowed an accurate determination of the column density of neutral hydrogen (H I), redshifted to optical wavelengths. The better resolution of the WHT spectra meant an accurate study of metal lines in the spectrum was possible. A large number of metal lines are found in the spectra, including (forbidden) fine-structure lines. Based on the

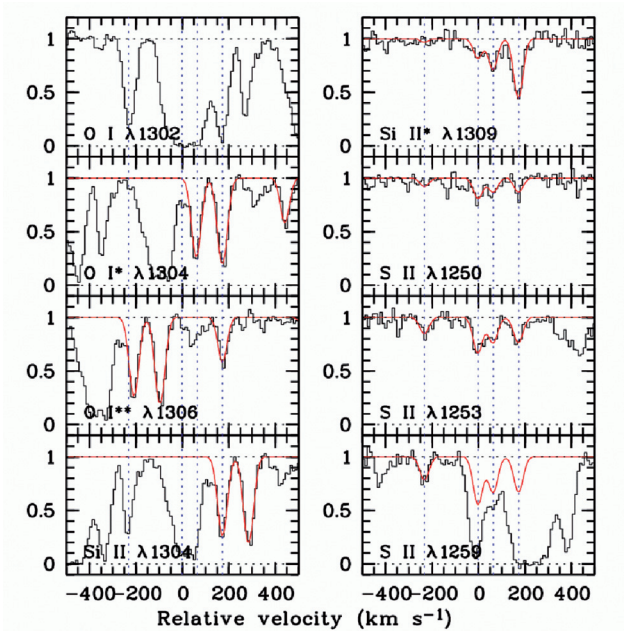

Figure 35. Portions of the ISIS spectrum showing the OI, OI, OI**, SiII, SiII* and SII lines. It is clearly visible that there are four discrete velocity components, with velocity differences of up to ~500 km s^{-1}.*

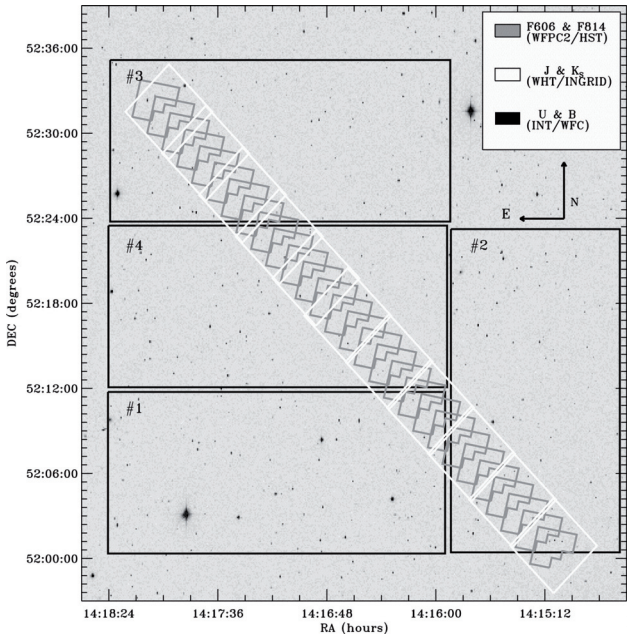

Figure 36. Observations of the GOYA Survey in the GWS region over a DSS image. The 28 HST WFPC2 pointings defining the GWS in F606W and F814W are shown in gray, while J and Ks WHT INGRID fields are shown in white. The GWS runs diagonally across the wide 45'×45' field marked in black, which corresponds to the INT WFC field (U and B data). Numbers in black indicate positions and orientations of the four chips of WFC (figure from Eliche-Moral et al., 2006, ApJ, 639, 644).

measurement of the neutral hydrogen column density and the metal content from weak, unsaturated singly-ionised sulphur (S II) lines, a metallicity of [S/H] = –0.84 ± 0.10, or ~0.14 times solar metallicity, was derived. This is in fact one of the highest metallicities measured from absorption lines at redshift around 4. From the very high column densities for the forbidden singly-ionised silicon (Si II*), and neutral oxygen (O I* and O I**) lines, the researchers infer very high densities in the system, significantly larger than 10^4 cm^{-3}.

The high-resolution spectra also allow the astronomers to study the kinematics of the absorption systems. Several different, discrete velocity systems can be distinguished, with velocities of up to 500 km s^{-1}. Most surprisingly however, was the tentative detection of molecular hydrogen in the ISIS spectrum. This is the very first detection of molecular lines in an optical GRB afterglow spectrum. Especially remarkable is the fact that this possible detection has been achieved with a 4-metre telescope, proving that medium size telescopes can compete when response times are short.

U AND *B* NUMBER COUNTS FROM THE GOYA SURVEY

The Galaxy Origins and Young Assembly (GOYA) survey is designed to study the formation and evolution of galaxies with the aim of learning about the epoch and the mechanisms by which galaxies assembled the bulk of their stars and acquired their present structure and dynamics. For this, a near-infrared/optical observational program using some of the most powerful ground-based telescopes and public data is being conducted to map 0.5 square degrees of high-latitude sky. As the main scientific motivation behind the design of EMIR (a NIR cryogenic multi-slit spectrograph for the 10.4m GTC at Observatorio del Roque de los Muchachos), GOYA emphasizes the use of near-infrared observations, which sample the optical rest-frame spectrum of galaxies at very high redshifts.

The GOYA photometric survey is a multicolour survey in six broadband filters (*U*, *B*, *V*, *I*, *J*, K_s) with target depths of *U*=*B*=*V*=*I*=26 and *J*=*K*=22 (AB magnitudes). Its principal aim is to generate a galaxy database for sample selection and characterisation for subsequent NIR spectroscopy with EMIR.

The *U* and *B* imaging came from observations carried out with the INT Wide Field Camera and covers the Groth-Westphal Strip (GWS). The GOYA Survey has also reduced and analysed data over this field in NIR filters from WHT INGRID (J and Ks) and in visible filters from HST WFPC2 (F606W and F814W). Originally, the GWS field

was defined as 28 HST WFPC2 pointings extended along a 45' strip. It has an area of ~150 arcmin^2 of sky. Compared to other existing optical-NIR surveys, GOYA offers a notable increase in the depth times area product in several filters, compiling complementary photometry in six optical-NIR bands and morphological and surface brightness information from high-resolution HST WFPC2 images.

Counts were derived over the magnitude ranges $18.0<U<25.0$ and $19.5<B<25.5$. These wide ranges (7 magnitudes in *U* and 6 magnitudes in *B*) result from the combination of wide area and depth of the survey. In both bands, the number counts are in good agreement with other studies that cover fainter and brighter magnitudes. When combined with K_s number counts, the data provide strong constraints on galaxy formation models, due to the presence of a knee at K_s=17.5 in the NIR counts and the absence of such a feature in blue passbands.

Adopting a Λ-dominated cosmological model, a simple number count model (including luminosity evolution and a galaxy number evolution) accurately reproduces the observed counts in *U*, *B* and K_s in a consistent way. Extensive modelling suggests that only by assuming a moderately low formation redshift for the dominant NIR population (elliptical galaxies) does the model reproduce the K_s=17.5 knee. Reproducing the lack of a knee in the *U* and *B* counts, subsequently requires the adoption of a moderate optical depth for all galaxy types, including elliptical galaxies. Neither of the two assumptions are at odds with current ideas on galaxy formation and evolution in hierarchical universes.

THE STAR FORMATION RATE AT REDSHIFT ONE

The quest for giving the first global view of the history of star formation in the Universe, as a key element in understanding galaxy assembly, commenced around 10 years ago. To date, many quantitative attempts to measure the global star formation history have been based on optical measurements and have thus suffered from having to use different indicators of star formation in various redshift bins, redshifted into the optical.

These various indicators not only have uncertain relative calibrations but are also affected differently by dust extinction. Commonly used star formation rate (SFR) indicators are ultraviolet (UV) continuum luminosity, which can be heavily dust extinguished, and nebular emission lines such as H alpha and [O II], (the latter of which is strongly dependent on metallicity and ionisation state). Longer wavelength estimators relying on far-infrared (FIR) or radio luminosity are insensitive to dust obscuration and yet have their own caveats.

The Universe at redshift z~1–2 is believed to be one of the most active epochs in galaxy formation and evolution. Indeed, it is inferred to be the epoch at which large elliptical and spiral galaxies are assembled and therefore may also be the period of peak star formation in the Universe. Yet, the Universe at this epoch is still neither well studied, nor well understood. Observations have long been hampered by the difficulties of observing objects at these redshifts in the visible wavebands. At redshift z~1, key diagnostic spectral features are redshifted out of the optical into the near-infrared (near-IR), which is a difficult regime to work in, and the rest UV Lyman alpha line is not accessible in the optical until around redshifts z~2.5. The redshift range z~1–2 has hence traditionally been dubbed the spectroscopic 'redshift desert'. Furthermore, there is certainly evidence that the SFR was much higher in the recent past (z~0.5), compared to the current epoch. However, it is still unclear whether at redshifts of one and beyond, the star formation density plateaus, declines, or perhaps continues to increase.

A team of astronomers have used the Cambridge Infrared Panoramic Survey Spectrograph (CIRPASS) mounted on the WHT with the aim of addressing the true star formation history of the Universe at redshifts z= 0.7–1.5 , through H alpha measurements of a large sample of galaxies. CIRPASS is a near-IR fibre-fed spectrograph operating between 0.9 and 1.67 μm and it can operate with 150 fibres with the ability to simultaneously observe up to 75 targets (in object/sky pairs). CIRPASS work with one of two modes – with an Integral Field Unit or in multi-object mode (CIRPASS-MOS). CIRPASS-MOS was used at the Cassegrain focus of the WHT to observe 62 objects at a time in the Hubble Deep Field-North. The fibre size corresponds to ~1.1 arcsec at the WHT (which is approximately comparable to the expected seeing convolved with typical galaxy profiles, at least for compact galaxies). CIRPASS-MOS demonstrates a powerful new technique for studying distant galaxies, and this is the first successful example of near-IR multi-object spectroscopy of high-redshift galaxies.

Stacking the spectra in the rest frame, to infer a total SFR for the field, they find a lower limit (uncorrected for dust reddening) on the SFR density at redshift z= 1 of 0.04 solar masses per year and Mpc^{-3}. This implies rapid evolution in the SFR density from z=0 to 1 which is proportional to $(1+z)^{3.1}$.

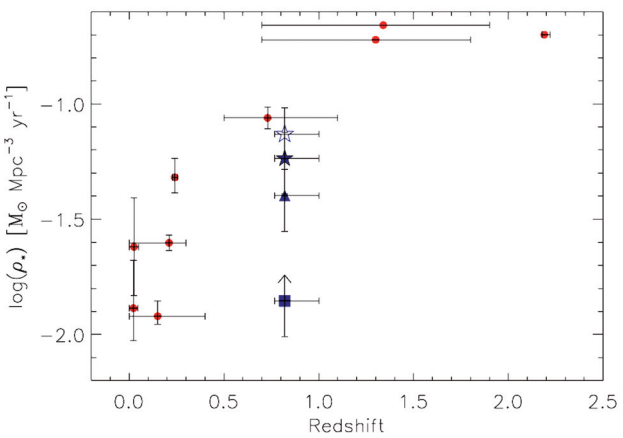

Figure 37. Star formation rate densities determined from Hα measurements only and with reddening corrections. The authors used their own reddening corrections where applicable. The uncorrected data points are shown with a square and triangle. Reddening-corrected points are shown for the Milky Way law (filled star) and a Calzetti law (open star) (figure from Doherty et al., 2006, MNRAS, 370, 331).

This successful application of multi-object fibre spectroscopy to observe high-redshift galaxies constitutes a powerful technique, and the success of this multi-object spectroscopic survey bodes well for larger surveys with future instruments such as EMIR on Gran Telescopio Canarias.

DISCOVERY OF THE MOST MASSIVE GALAXY LENS

There have been many optical giant arcs discovered, caused by the lensing effects of massive galaxy clusters and their central galaxies. But, few optical rings have ever been found, despite theoretical predictions that they should be abundant.

Using data from the Sloan Digital Sky Survey (SDSS) Data Release 5 (DR5), astronomers found the largest optical Einstein ring known, an almost complete (~300°) Einstein ring of diameter 10.2", more than 5 times the size of previously-known optical rings. Further imaging follow-up with the Wide Field Camera on the INT revealed a "horseshoe" shape with three brightness peaks, and thus the name "Cosmic Horseshoe".

The lensing galaxy itself is an interesting object, it is a member of a rare population of Luminous Red Galaxies (LRGs). These are the largest and most massive galaxies in the universe, and they are also believed to host massive black holes. This deflecting galaxy has a line-of-sight

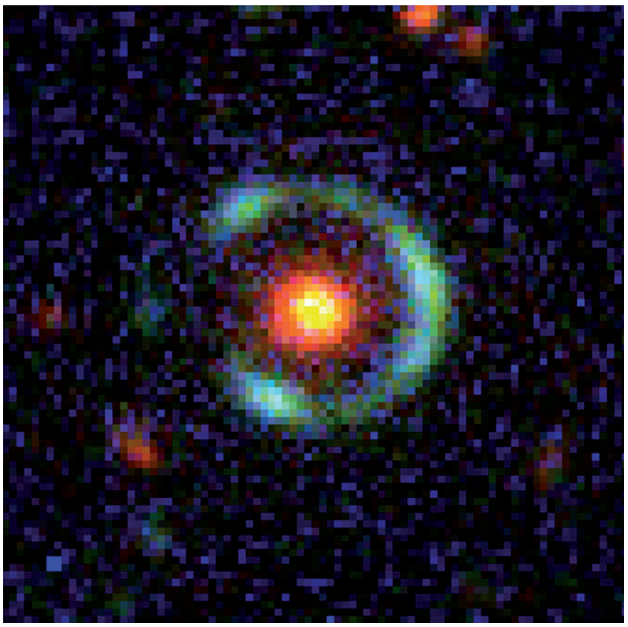

Figure 38. INT WFC u, g, i composite of the Cosmic Horseshoe from follow-up data (figure from Belokurov et al., 2007, ApJ, 671, L9)

velocity dispersion in excess of 400 km s^{-1} and a redshift of 0.444, while the source is a star-forming galaxy with a redshift of 2.379. From its colour, luminosity, and velocity dispersion, they argue that this is the most massive galaxy lens hitherto discovered.

OTHER SCIENTIFIC HIGHLIGHTS BRIEFLY

The kinematics of diffuse ionised gas in the disk halo interface of NGC 891

The properties of the gas in halos of galaxies constrain global models of the interstellar medium. Kinematical information is of particular interest since it is a clue to the origin of the gas. From Fabry-Pérot TAURUS II observations at the WHT of the kinematics of the thick layer of the diffuse ionised gas in NGC 891, the rotation curve of the halo gas could be determined. Hα data cubes show much higher angular resolution than in the H I 21cm line. The velocity information of the diffuse ionised gas extracted from the data cube is compared to model distributions to constrain the distribution of the gas and in particular the halo rotation curve. The astronomers find that the scale length of the H alpha must be between 2.5 and 6.5 kpc. Furthermore they find evidence that the rotation curve above the plane rises less steeply than in the plane. This is all in agreement with the velocities measured in the H I (Kamphuis et al., 2007, *A&A*, 468, 451).

The European Galactic Plane Surveys (EGAPS): IPHAS and UVEX

The European Galactic Plane Surveys (EGAPS) will, for the first time ever, map the complete galactic plane , (10×360 degrees), down to 21st magnitude in u', g', r', i' and H alpha and partly in He I 5875. It will complete a database of ~1 billion objects. The aim of EGAPS is to study populations of short-lived stellar and binary phases in our Galaxy and combine these population studies with stellar and binary evolutionary codes to vastly improve our understanding of crucial phases of stellar evolution. Target populations include Wolf-Rayet stars, planetary nebulae, white dwarfs (in binaries), cataclysmic variables and other mass-transferring binaries. EGAPS uses the INT+WFC for the Northern Hemisphere and will use the VST+Omegacam in the Southern Hemisphere. The Northern red survey (IPHAS, using r', i', and Halpha) started in 2003 and is complete. The northern blue survey (UVEX; u',g',r' and HeI) started in June 2006. Early results include the detection of a number of rare planetary nebulae, cataclysmic variables, red-dwarf white-dwarf binaries in clusters, a possible AM CVn candidate, and a deep photometric and spectroscopic investigation of the Cyg X region. EGAPS will revolutionise the field of galactic stellar astrophysics by completing the first ever fully digital, multicolour deep survey of the Galactic Plane (Groot et al, 2006, 26th meeting of the IAU, Joint Discussion, 13, 54.).

Kinematics of the ultracompact helium accretor AM Canum Venaticorum

AM Canum Venaticorum stars (AM CVn stars in short) are interacting binary stars whose mass, mainly helium, is constantly flowing from one star to the other. What makes these objects special is their ultra-compact nature.They consist of two degenerate, hydrogen-deficient stars, which means that these binaries have extremely short orbital periods, from about one hour down to only a few minutes. Their ultracompact nature makes them the strongest known sources of gravitational waves that can potentially be detected with the future ESA/NASA cornerstone satellite mission LISA, the Laser Interferometer Space Antenna. Until now, only a few exotic AM CVn stars were known. Of crucial importance for expanding the known population has been the advent of wide-field surveys such as the SDSS. In order to further improve the statistics of the sample, a number of dedicated wide-field sky surveys were designed and started, among them, IPHAS and UVEX on the INT. In addition to population studies, some astronomers embarked on a project to study individual systems in detail, using phase-resolved spectroscopic techniques. One of the main questions to address was how these binaries are formed. Theoretically, no fewer than three different formation channels have been proposed to contribute to the AM CVn population, but which of these channels actually produce AM CVn stars, and in what numbers, has been a long-standing problem.

Using ISIS on the WHT, a team of astronomers was able to weigh the stars of the AM CVn binary, and showed that they are more massive than previously thought. This has important consequences for their formation and evolution. In addition, these observations allowed them, for the first time, to accurately predict the gravitational-wave signatures of these binary stars and they have shown that the known short-period AM CVn stars are the first solid candidates for detection with a LISA-type instrument. These stars will thus be of crucial importance to test and calibrate such a gravitational-wave detector, as well as directly test the predictions from General Relativity concerning the emission of gravitational waves from binary stars (Roelofs et al., 2006, MNRAS, 371, 1231).

A composite H II region luminosity function in Hα of unprecedented statistical weight

Statistical properties of H II region populations in disk galaxies yield important clues to the physics of massive star formation. Previous studies have shown that there might exist a dual slope in the luminosity function (LF) of H II regions, with a well defined break at a specific luminosity, but the lack of a sufficient statistical base has prevented a conclusive result. One approach can be increasing the statistical weight by deriving a general form of the LF from

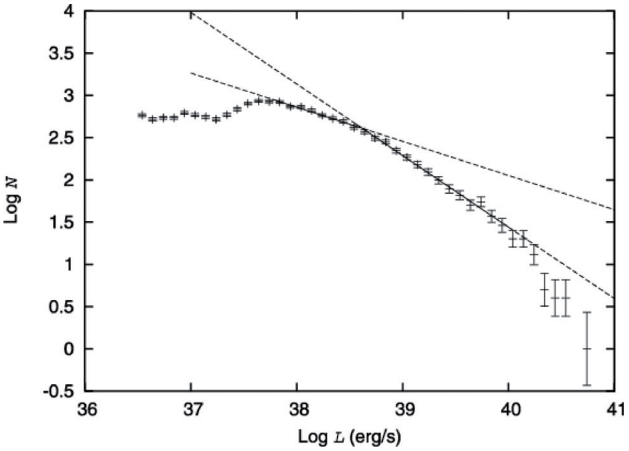

Figure 39. LF made from the combined H II region catalogues of 53 nearby spiral galaxies. The large number of H II regions allows plotting the LF in steps of 0.1 dex. The best double-slope fit is indicated by the lines, where dashes show extrapolations beyond the range over which the best fit has been made (figure from Bradley et al., 2006, A&A, 459, L13).

a sample of nearby spiral galaxies. For this reason, a team of astronomers obtained Hα images of a sample of 53 spiral galaxies using the JKT, and after photometric calibration, the galaxies were summed to form a total LF comprising 17,797 H II regions. The new LF shows a clear two slope power law behaviour, with a significantly steeper slope for the high luminosity branch. This can be modelled by assuming that the high luminosity regions are density bounded, though the scenario is complicated by the inhomogeneity of the ionised interstellar medium. The break, irrespective of its origin, is of potential use as a distance indicator for disc galaxies (Bradley et al., 2006, A&A, 459, L13).

Massive star formation in the central regions of spiral galaxies

Enhanced nuclear activity in disk galaxies, in starburst or AGN form, appears to be an integral part of their evolution. Both forms of activity have been observed to co-exist and are a clear manifestation of the symbiotic evolution of galactic centres and their host galaxies. The observed tight correlation between the masses of the central black holes and the velocity dispersions in the surrounding bulges provides the most direct evidence for this evolution and yields important clues on the dynamics, structure, and evolution of galaxies.

To initiate and to maintain the AGN or nuclear starburst activity, gas inflow must be stimulated from the disk to the central regions – a process which must be accompanied by a substantial loss of angular momentum in the gas. Theoretically, this leads to the suggestion that gravitational torques acting through galactic bars or galaxy interactions are involved. Massive star formation can be convincingly traced by the accompanying Hα emission and is very easily observed with standard telescopes and cameras. Hα is mainly produced in the H II regions surrounding massive B and O stars, although shocks and non-stellar activity can also lead to Halpha emission.

Using 73 images of galaxies obtained with the AUX camera of the WHT, a team of astronomers studied the morphology of the Hα emission in the circumnuclear, two kpc radius regions, as well as from the nucleus *per se*. The circumnuclear area that was chosen is large enough to incorporate most nuclear rings. For most of the galaxies, no Hα imaging was available and the spatial resolution was mostly below one second of arc. They confirmed that late-type galaxies have a patchy circumnuclear appearance in Hα, and that nuclear rings occur primarily in spiral types Sa-Sbc. They identified a number of previously unknown nuclear rings, and confirmed that nuclear rings are predominantly hosted by barred galaxies. Other than stimulating nuclear rings, bars do not influence the relative strength of the nuclear Hα peak, nor the circumnuclear Hα morphology. No significant influence of the presence or absence of a close companion on the relative strength of the nuclear Hα peak, nor on the Hα morphology around the nucleus, was found (Knapen et al., 2006, A&A, 448, 489; Sarzi et al., 2007, MNRAS, 380, 949).

The water ice rich surface of (145453) 2005 RR43: a case for a carbon-depleted population of TNOs?

Spectroscopic and spectrophotometric studies show that about 70% of Trans-Neptunian Objects (TNOs) present a mantle of complex organics on their surfaces. Long term processing by high energy particles and solar radiation on icy bodies, induces the formation of organic species in their outer layers, resulting in a mantle that covers the unprocessed original ices. Until recently, the only case of a TNO with a surface covered basically by a thick layer of water ice was Charon, and it has been considered an intriguing case because of the need of a resurfacing mechanism like cryovolcanism or collisions with micro-meteorites. Recently, it has been showed that other TNOs also have surface composition similar to Charon and are located in a narrow region of the orbital parameters space. The existence of a population of TNOs with Charon-like surfaces and similiar orbital parameters needs to be explained, as it can have a strong impact on the knowledge of the trans-neptunian belt formation theories and/or resurfacing mechanisms. A study of the surface composition of the TNO (145453) 2005 RR43 using ISIS on the WHT showed that this object is indeed a member of such a population (Pinilla-Alonso et al., 2007, A&A, 468, L25).

DE CVn: a bright, eclipsing red dwarf-white dwarf binary

Large gaps remain in our knowledge of binary stellar evolution that not only affect our understanding of evolved compact binaries, but also of phenomena such as supernovae type Ia explosions, the rate of mergers between neutron stars, and the number of gravitational wave sources in our Galaxy. The poorly understood physics of the common-envelope (CE) phase results in considerable uncertainty in binary evolution models. During the evolution of a binary, the more massive star turns into a giant. When the initial orbital period is small enough, the envelope of the giant will encompass the secondary star. The secondary and the core of the giant will spiral in towards each other in a CE. When the envelope is expelled, a close binary, consisting of the core

of the giant (which will evolve towards a white dwarf) and the unevolved secondary star may emerge. The CE phase is expected to be very short, lasting less than ~1000 years, and therefore is virtually impossible to observe directly.

To study the effects of this phase, it is best to focus on objects that have most probably undergone a CE phase in their past. These are identified with binary systems containing at least one stellar remnant, where the current orbital separation is smaller than the radius of the giant progenitor, usually with orbital periods shorter than 1 day. Close white dwarf-red dwarf binaries must have passed through a common-envelope phase during their evolution. DE CVn is a detached white dwarf-red dwarf binary with a relatively short (~8.7 h) orbital period. Its brightness and the presence of eclipses make this system ideal for a more detailed study. From photometric and spectroscopic observations of DE CVn using ULTRACAM and ISIS on the WHT among other instruments, a team of astronomers found that the mass of the white dwarf is 0.51 solar masses, its effective temperature is 8000 K, and it has a hydrogen-rich atmosphere (DA-type). The red dwarf has a spectral type of M3V and its mass is 0.41 solar masses. The astronomers reconstructed its evolution and found that the progenitor of the white dwarf was a relatively low-mass star of less than 1.6 solar masses. The current age of this system is $3.3\text{-}7.3\times10^9$ years, while it will take longer than a Hubble time for DE CVn to evolve into a semi-detached system (van den Besselaar et al., 2007, A&A, 466, 1031).

Echoes from the companion star in Sco X-1

When the accreting compact object in an interacting binary is a neutron star or a black hole, the potential well is so deep that the infalling gas is heated to more than a million degrees Kelvin, producing abundant X-rays. These objects are therefore called X-ray binaries, and part of the observational work has concentrated on the so-called ultra-compact X-ray binaries (UCXBs). They are the X-ray binary cousins of the AM CVn stars and are also promising sources of gravitational wave radiation.

Low-mass X-ray binaries (LMXBs) are interacting binaries containing a low-mass donor star transferring matter on to a neutron star or black hole. Mass accretion takes place through an accretion disc, and with temperatures approaching ~10^8 K. In these binaries optical emission is dominated by reprocessing of the powerful X-ray luminosity in the gas around the compact object which usually swamps the spectroscopic features of the weak companion stars. In this scenario, dynamic studies have classically been restricted to the analysis of X-ray transients during quiescence, where the intrinsic luminosity of the donor dominates the light spectrum of the binary.

Sco X-1 is the prototype LMXB and also the brightest persistent X-ray source in the sky and it has been the target of detailed studies since its discovery. Simultaneous X-ray and ULTRACAM optical data of Sco X-1 were obtained to cover the full 18.9-h orbital period in 12 snapshots, yielding 16.1 ks of X-ray data and simultaneous optical photometry in three different bands. For the first time, astronomers were able to isolate the emission line contributions from the mass donor star that correspond to X-ray variations with a delay that is consistent with the light travel time between the X-ray source near the neutron star and the irradiated face of the donor star that directly contributes to the emission (Muñoz-Darias et al., 2007, MNRAS, 379, 1637).

Searching for the lowest mass galaxies: an HI perspective

In the currently favoured cosmological models, structure evolves, by gravitational instability, from small, primordial, fluctuations in the dark-matter distribution. In this framework, galaxies form by the cooling of gas captured inside the dark-matter halos. In normal-sized galaxies, this cool gas will form stars, making the galaxy visible in optical light. However, various physical processes may prevent the cooling of the gas, and therefore the formation of stars. Such halos would remain dark in optical light. One possibility is that small galaxies are not heavy enough to condense the gas to densities high enough for star formation to occur. It may also be the case that the radiation of the first large objects formed in the universe keeps the gas in small galaxies ionised. Finally, it is conceivable that if a few stars form in a small galaxy, supernovae will expel the remaining gas, halting further star formation.

One possibility to test these various hypotheses is to study the neutral gas content of very small galaxies. The various theories about what may happen to the gas when small galaxies form, make different predictions for the gas content. For example, if all the gas is expelled, there may be a lower limit to the size of galaxies. On the other hand, if galaxies are too small to compress the gas so that stars can form, one should find very small galaxies that are dark in the optical but are detectable in neutral hydrogen because they consist solely of gas. Such systems are dubbed "dark galaxies".

So far, blind extragalactic surveys of neutral hydrogen have failed to detect a population of dark galaxies.

However, this may be due to these surveys not being sensitive to objects smaller than 10^{7}-^{8} solar masses of H I and hence they may not be able to find the small, dark H I clouds predicted by some theories. To answer the question of whether a significant population of gas-rich, low-luminosity, low-surface brightness, or even dark galaxies, exist, it is necessary to reach lower H I masses. In order to achieve this, a new blind H I survey using the WSRT telescope of 90 square degrees in the constellation of Canes Venatici (the so-called "CVn survey") was designed to be sensitive to objects with HI masses down to below 10^{6} solar masses.

To be able to study the optical properties of the detections, the smaller galaxies were also observed with the INT WFC where images of the objects were made in different colours. These observations show that all objects detected in H I have clear counterparts in the optical. Therefore, the data do not give any indication that, even when going to lower H I masses, dark H I objects exist (Kovac, 2007, "Searching for the lowest mass galaxies: an H I perspective", PhD thesis, Rijksuniversiteit Groningen; Kovac et al, 2005, "The faint end of the H I mass function", IAU Colloquia, 198, 351).

The ING Override Programme and Gamma-Ray Bursts

The ING Override Programme continues to produce a significant number of papers, in particular in the field of Gamma-Ray Bursts. During 2006 and 2007, the following papers were published using data from a wide variety of instruments (PFIP, LIRIS, ISIS, INGRID, AUX and WFC): Castro-Tirado et al., 2006, “GRB 051028: an intrinsically faint gamma-ray burst at high redshift?", A&A, 459, 763; De Ugarte Postigo et al., 2006, “GRB 060121: Implications of a Short-/Intermediate-Duration Gamma-Ray Burst at High Redshift", ApJ, 648, L83; Fynbo et al., 2006, “Probing cosmic chemical evolution with gamma-ray bursts: GRB 060206 at z = 4.048", A&A, 451, L47; Levan et al., 2006, “Infrared and Optical Observations of GRB 030115 and its Extremely Red Host Galaxy: Implications for Dark Bursts", ApJ, 647, 471; Castro-Tirado et al., 2007, “The dark nature of GRB 051022 and its host galaxy", A&A, 475, 101; Ruiz-Velasco et al., 2007, "Detection of GRB 060927 at z = 5.47: Implications for the Use of Gamma-Ray Bursts as Probes of the End of the Dark Ages", ApJ, 669, 1; Curran et al., 2007, “GRB 060206 and the quandary of achromatic breaks in afterglow light curves", MNRAS, 381, L65).

New Milky Way Companions

The known satellite galaxies of the Milky Way all lie within ~300 kpc, and their brightest stars are resolvable from ground-based telescopes. Thus, it is possible to acquire an enormous wealth of data on their stellar populations, making the satellite galaxies important objects in many fields of astrophysics. They have also emerged as a battleground in near-field cosmology. Using data from the SDSS, astronomers have found 5 new satellites of the Milky Way, one of which was followed-up with the Wide Field Camera on the INT. So far astronomers accept 14 mini-galaxies as Milky Way satellites, (the dwarf irregulars, Large and Small Magellanic Clouds and 12 dwarf spheroidals), although sometimes the distinction between star clusters and dwarf galaxies is ambitious. The possible disrupting satellites, Canis Major and Virgo, overdensities and the already absorbed dwarf known as the Monoceros Ring, are other structures related to this research (V. Belokurov et al., 2007, "Cats and Dogs, Hair and a Hero: A Quintet of New Milky Way Companions", ApJ, 654, 897).

Discovery of a cluster of galaxies behind the Milky Way

Rich clusters of galaxies have been successfully used as tracers of large-scale structure formation and evolution, which has allowed the setting of constraints on various cosmological parameters. In the past, the majority of rich clusters was first identified in the optical and later observed in X-rays. However, with the advent of large and deep X-ray surveys, X-ray observations have become one of the most useful techniques for discovering clusters of galaxies, especially for intermediate and high-redshift systems. On the other hand, X-rays may also be useful for detecting clusters near the Galactic plane, where the increasing number of stars and extinction makes the optical identification of background galaxies difficult. Following this approach, astronomers reported the discovery of Cl 2334+48, a rich cluster of galaxies in the Zone of Avoidance, identified in public images from the XMM-Newton archive, and followed up using optical images with the Wide Field Camera on the INT (Lopes de Oliviera et al., 2006, "Discovery of a cluster of galaxies behind the Milky Way: X-ray and optical observations", A&A, 459, 415).

The RApid Temporal Survey (RATS)

The intensity of stellar objects can vary on a wide range of time-scales, ranging from seconds to months to years. A large number of projects now exist whose aim is to detect such varying sources. The reasons for this are many, but include the search for extrasolar planets and interacting binary stars. Most of these surveys are sensitive to time-scales longer than a day. It is only recently that such surveys have been sensitive to shorter term time-scales. For instance, the Faint Sky Variability Survey on the INT

has a large survey area and it was sensitive to variations only as short as ~24 min. In principle the SuperWasp project is sensitive to variations on time-scales as short as a few minutes. However, it is sensitive to relatively bright objects, V~7–15 .

Why is it important that we extend the parameter search down to periods shorter than 10 min? Recently a new class of object has been discovered in which coherent intensity variations have been detected on time-scales of ~10 min or less. It is thought that these systems are interacting white dwarf–white dwarf pairs which have no accretion disc, and the observed period represents the binary orbital period. As such, they are expected to be amongst the first sources to be detected using LISA, the planned gravitational wave observatory.

These systems are at the short end of the period distribution of white dwarf–white dwarf binaries, or AM CVn systems. For orbital periods less than 80 min, the secondary (mass-donating) star cannot be a main-sequence star. Furthermore, for periods shorter than 30 min, the secondary must be a helium white dwarf.

The aim of the RApid Temporal Survey (RATS) is to discover objects whose optical intensity varies on time-scales of a few minutes to several hours. The prime aim is to discover interacting ultracompact binary systems – systems consisting of two degenerate (or semi degenerate) stars orbiting around a common centre of gravity – with binary orbital periods of less than ~70 min. The pilot survey data was obtained using the INT and the Wide Field Camera. It covered 3 deg^2 and reached a depth of *V*~22.5. Nearly 50 sources were found to show significant intensity variations and none were previously known variable objects. However, only four objects showed modulations which varied on periods of approximately 1 h or less, one being a subdwarf B star and the other three are likely to be SX Phe stars. (Ramsay and Hakala, 2005, "RApid Temporal Survey (RATS) – I. Overview and first results", MNRAS, 360, 314; Ramsay et al., 2006, "RApid Temporal Survey (RATS) – II. Followup observations of four newly discovered short-period variables", MNRAS, 371, 957).

Exploration of the Kuiper Belt by High-Precision Photometric Stellar Occultations: First Results

Astronomers report the first detection of hectometre-size objects by the method of serendipitous stellar occultation using ULTRACAM on the WHT. This method consists of recording the diffraction shadow created when an object crosses the observer's line of sight and occults the disk of a background star. One of the detections is most consistent with an object between Saturn and Uranus in size. The two other diffraction patterns detected were caused by Kuiper Belt objects beyond 100 AU from the Sun and hence are the farthest known objects in the solar system. These detections show that the Kuiper Belt is much more extended than previously believed and that the outer part of the disk could be composed of smaller objects than the inner part. This gives critical clues to understanding the problem of the formation of the outer planets of the solar system (Roques et al., 2006, "Exploration of the Kuiper Belt by High-Precision Photometric Stellar Occultations: First Results", AJ, 132, 819).

The MEGA survey

The Microlensing Exploration of the Galaxy and Andromeda (MEGA) survey uses several instruments and telescopes, among them, the Wide Field Camera on the INT, to detect microlensing towards the nearby Andromeda galaxy, M 31, in order to establish whether massive compact objects are a significant contribution to the total mass budget of the dark halo of M 31. The MEGA observations with the INT spanned four observing runs in the first three seasons. The data were acquired jointly with the POINT-AGAPE collaboration although the data reduction and analysis were performed independently. Using a fully automated search algorithm, astronomers identified 14 candidate microlensing events. The results from the survey are compared with theoretical predictions for the number and distribution of events. For most models, the observed event rate is consistent with the rate predicted for self-lensing - a MACHO halo fraction of 30% or higher can be ruled at the 95% confidence level. The event distribution does show a large near-far asymmetry, hinting at a halo contribution to the microlensing signal. Two candidate events are located at particularly large projected radii on the far side of the disk. These events are difficult to explain by self-lensing and only somewhat easier to explain by MACHO lensing. A possibility is that one of these is due to a lens in a giant stellar stream. (J. T. A. de Jong et al., 2004, "First microlensing candidates from the MEGA survey of M 31", A&A, 417, 461; J. T. A. de Jong et al., 2006, "MACHOs in M 31? Absence of evidence but not evidence of absence", A&A, 446, 855).

The Angstrom Project Alert System

The Angstrom Project is undertaking an optical survey of stellar microlensing events across the bulge region of the Andromeda galaxy (M 31), using a distributed network of

2-m class telescopes, among them, the INT and the Wide Field Camera. The Angstrom Project Alert System (APAS) was developed to identify candidate microlensing and transient events in real time, using data from robotic telescopes. This is the first time that real-time microlensing discovery has been attempted outside of the Milky Way and its satellite galaxies. The APAS is designed to enable follow-up studies of M31 microlensing systems, including searches for gas giant planets in M31, and other transient events. In addition to the new observing data, the APAS uses archive data from the POINT-AGAPE dark matter microlensing survey of M31 (M. J. Darnley et al., 2007, "The Angstrom Project Alert System: Real-Time Detection of Extragalactic Microlensing", ApJ, 661, L45).